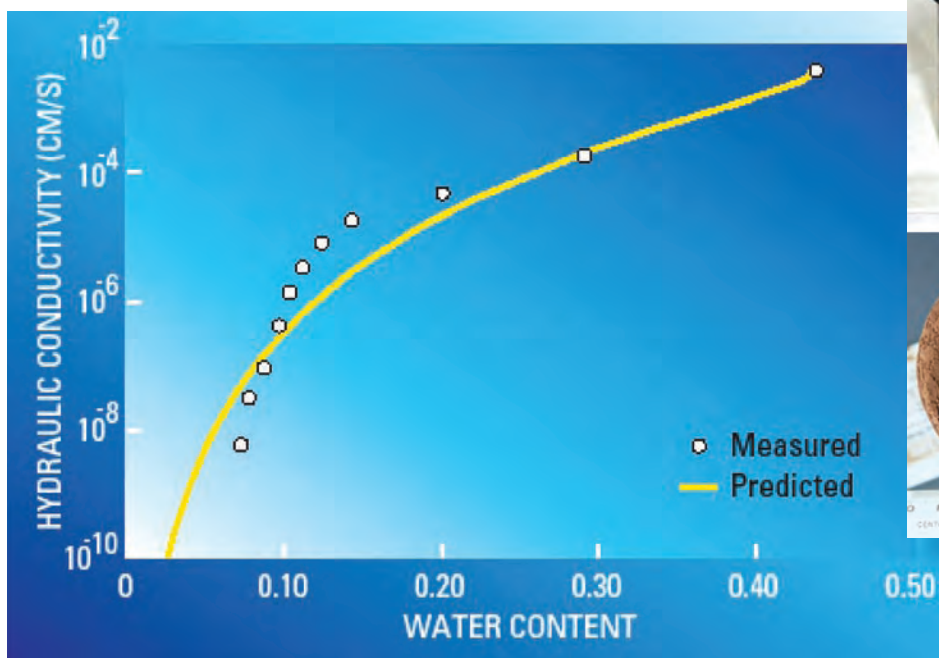


DOE/ID-22202

Prepared in cooperation with the U.S. Department of Energy

# Property-Transfer Modeling to Estimate Unsaturated Hydraulic Conductivity of Deep Sediments at the Idaho National Laboratory, Idaho



Scientific Investigations Report 2007–5093

**Cover:** Graph showing example of measured and estimated hydraulic conductivity [ $K(\theta)$ ] curves.  
(Photographs of core samples used to develop property transfer models courtesy of Kim S. Perkins,  
U.S. Geological Survey.)

# **Property-Transfer Modeling to Estimate Unsaturated Hydraulic Conductivity of Deep Sediments at the Idaho National Laboratory, Idaho**

By Kim S. Perkins and Kari A. Winfield

Prepared in cooperation with the  
U.S. Department of Energy

Scientific Investigations Report 2007–5093

**U.S. Department of the Interior**  
**U.S. Geological Survey**

**U.S. Department of the Interior**  
DIRK KEMPTHORNE, Secretary

**U.S. Geological Survey**  
Mark D. Myers, Director

U.S. Geological Survey, Reston, Virginia: 2007

For product and ordering information:

World Wide Web: <http://www.usgs.gov/pubprod>

Telephone: 1-888-ASK-USGS

For more information on the USGS--the Federal source for science about the Earth, its natural and living resources, natural hazards, and the environment:

World Wide Web: <http://www.usgs.gov>

Telephone: 1-888-ASK-USGS

Any use of trade, product, or firm names is for descriptive purposes only and does not imply endorsement by the U.S. Government.

Although this report is in the public domain, permission must be secured from the individual copyright owners to reproduce any copyrighted materials contained within this report.

Suggested citation:

Perkins, K.S., and Winfield, K.A., 2007, Property-transfer modeling to estimate unsaturated hydraulic conductivity of deep sediments at the Idaho National Laboratory, Idaho: U.S. Geological Survey Scientific Investigations Report 2007-5093, 22 p.

# Contents

Abstract.....	1
Introduction.....	1
Site Description.....	3
Previous Investigations.....	3
Purpose and Scope .....	6
Hydraulic Conductivity Estimation Approach .....	6
Data Sets.....	8
Water-Retention Parameters and Hydraulic Conductivity Estimation.....	9
Results and Discussion.....	11
Root-Mean-Square Error Analysis .....	11
Parameter Testing With Numerical Simulation .....	15
Summary and Conclusions.....	20
Acknowledgments.....	20
References Cited.....	20

## Figures

Figure 1. Map showing locations of the Idaho National Laboratory, Idaho, and selected facilities .....	2
Figure 2. Maps showing locations of boreholes in the Radioactive Waste Management Complex, Idaho National Laboratory, Idaho, from which sedimentary interbed core samples were used to develop property-transfer models.....	4
Figure 3. Maps showing locations of boreholes in the Vadose Zone Research Park, Idaho National Laboratory, Idaho, from which sedimentary interbed core samples were used to develop property-transfer models .....	5
Figure 4. Diagram showing steps used to estimate unsaturated hydraulic conductivity .....	7
Figure 5. Diagram showing textural classification of core samples (based on the system of the U.S. Department of Agriculture [Soil Survey Staff, 1975]) used to evaluate property-transfer model for estimating unsaturated hydraulic conductivity $[K(\theta)]$ .....	8
Figure 6. Graph showing example of water-retention $[\theta(\psi)]$ curve showing components of the curve-fit model developed by Rossi and Nimmo (1994) .....	9
Figure 7. Graphs showing unsaturated hydraulic conductivity curves estimated using the RNJ-PTM- $K_{sat}$ model (property-transfer model-estimated saturated hydraulic conductivity and Rossi-Nimmo junction model parameters) .....	12
Figure 8. Graphs showing unsaturated hydraulic conductivity curves estimated using the RNJ-PTM model (laboratory-measured saturated hydraulic conductivity and property-transfer model-estimated Rossi-Nimmo junction model parameters) .....	12
Figure 9. Graphs showing unsaturated hydraulic conductivity curves estimated using the RNJ-CF model (laboratory-measured saturated hydraulic conductivity and Rossi-Nimmo junction model curve fits to measured water retention) .....	13

## Figures—Continued

Figure 10. Graphs showing unsaturated hydraulic conductivity curves estimated using the vG-CF model (laboratory-measured saturated hydraulic conductivity and van Genuchten model curve fits to measured water retention) .....	13
Figure 11. Graph showing comparison of root-mean-square errors in estimated hydraulic conductivity using RNJ-PTM- $K_{sat}$ model (property transfer model-estimated saturated hydraulic conductivity and Rossi-Nimmo junction model parameters); RNJ-PTM model (laboratory-measured saturated hydraulic conductivity and van Genuchten model curve fits to measured water retention) .....	14
Figure 12. Graph showing comparison between unsaturated hydraulic conductivity estimates from property-transfer models in terms of root-mean-square error and saturated hydraulic conductivity in terms of difference between measured and estimated values .....	14
Figure 13. Graphs showing water retention and hydraulic conductivity curves for core sample ICPP-SCI-V-215 (59.70 meter) illustrating the effect of few, clustered water-retention data points on the estimation of hydraulic conductivity .....	15
Figure 14. Graph showing comparison between goodness-of-fit of estimated water retention and goodness-of-fit of estimated unsaturated hydraulic conductivity in terms of root-mean-square error .....	15
Figure 15. Graphs showing water-retention and hydraulic-conductivity curves used in numerical simulations .....	17
Figure 16. Diagram showing results from VS2DT model numerical simulations for one-layer (left) and two-layer (right) systems using RNJ-PTM- $K_{sat}$ model (property transfer model-estimated saturated hydraulic conductivity and Rossi-Nimmo junction model parameters); RNJ-PTM model (laboratory-measured saturated hydraulic conductivity and property transfer model-estimated Rossi-Nimmo junction model parameters); RNJ-CF model (laboratory-measured saturated hydraulic conductivity and Rossi-Nimmo junction model curve fits to measured water retention); and vG-CF model (laboratory-measured saturated hydraulic conductivity and van Genuchten model curve fits to measured water retention) .....	19

## Tables

Table 1. Model variations used to estimate unsaturated hydraulic conductivity .....	7
Table 2. Core samples used to estimate unsaturated hydraulic conductivity in sedimentary interbeds underlying the Idaho National Laboratory, Idaho .....	8
Table 3. Ranges in number of measured unsaturated hydraulic conductivity points and average number of measured points for samples from three data sets used in the root-mean-square error analysis .....	11
Table 4. Parameter values used in numerical simulations for the one- and two-layer systems .....	16
Table 5. Root-mean-square error values for water retention and hydraulic conductivity used to describe sedimentary interbed material in numerical simulations for a one- and two-layer system .....	18

## Conversion Factors, Datums, and Acronyms

### Conversion Factors

<b>Multiply</b>	<b>By</b>	<b>To obtain</b>
centimeter (cm)	0.3937	inch
centimeter of water (cm-water)	0.01419	pound per square inch
centimeter per second (cm/s)	0.03281	foot per second
centimeter per day (cm/d)	0.03281	foot per day
cubic centimeter (cm <sup>3</sup> )	0.06102	cubic inch
kilometer (km)	0.6214	mile
meter (m)	3.281	foot
square kilometer (km <sup>2</sup> )	247.1	acre
square kilometer (km <sup>2</sup> )	0.3861	square mile

Temperature in degrees Celsius (°C) may be converted to degrees Fahrenheit (°F) as follows:

$$^{\circ}\text{F}=(1.8\times^{\circ}\text{C})+32.$$

### Datums

Vertical coordinate information is referenced to the National Geodetic Vertical Datum of 1929 (NGVD of 1929).

Horizontal coordinate information is referenced to the North American Datum of 1983 (NAD 83).

Altitude, as used in this report, refers to distance above the vertical datum.

### Acronyms

<b>Acronyms</b>	<b>Meaning</b>
ICPP	Idaho Chemical Processing Plant
INL	Idaho National Laboratory
INTEC	Idaho Nuclear Technology and Engineering Center
PTM	property-transfer model
RMSE	root-mean-square error
RNJ	Rossi-Nimmo junction model
RTC	Reactor Technology Complex
RWMC	Radioactive Waste Management Complex
SDA	Subsurface Disposal Area
SRP	Snake River Plain
TAN	Test Area North
TRA	Test Reactor Area
USGS	U.S. Geological Survey
VZRP	Vadose Zone Research Park

This page intentionally left blank.



# Property-Transfer Modeling to Estimate Unsaturated Hydraulic Conductivity of Deep Sediments at the Idaho National Laboratory, Idaho

By Kim S. Perkins and Kari A. Winfield

## Abstract

The unsaturated zone at the Idaho National Laboratory is complex, comprising thick basalt flow sequences interbedded with thinner sedimentary layers. Understanding the highly nonlinear relation between water content and hydraulic conductivity within the sedimentary interbeds is one element in predicting water flow and solute transport processes in this geologically complex environment. Measurement of unsaturated hydraulic conductivity of sediments is costly and time consuming, therefore use of models that estimate this property from more easily measured bulk-physical properties is desirable.

A capillary bundle model was used to estimate unsaturated hydraulic conductivity for 40 samples from sedimentary interbeds using water-retention parameters and saturated hydraulic conductivity derived from (1) laboratory measurements on core samples, and (2) site-specific property transfer regression models developed for the sedimentary interbeds. Four regression models were previously developed using bulk-physical property measurements (bulk density, the median particle diameter, and the uniformity coefficient) as the explanatory variables. The response variables, estimated from linear combinations of the bulk physical properties, included saturated hydraulic conductivity and three parameters that define the water-retention curve.

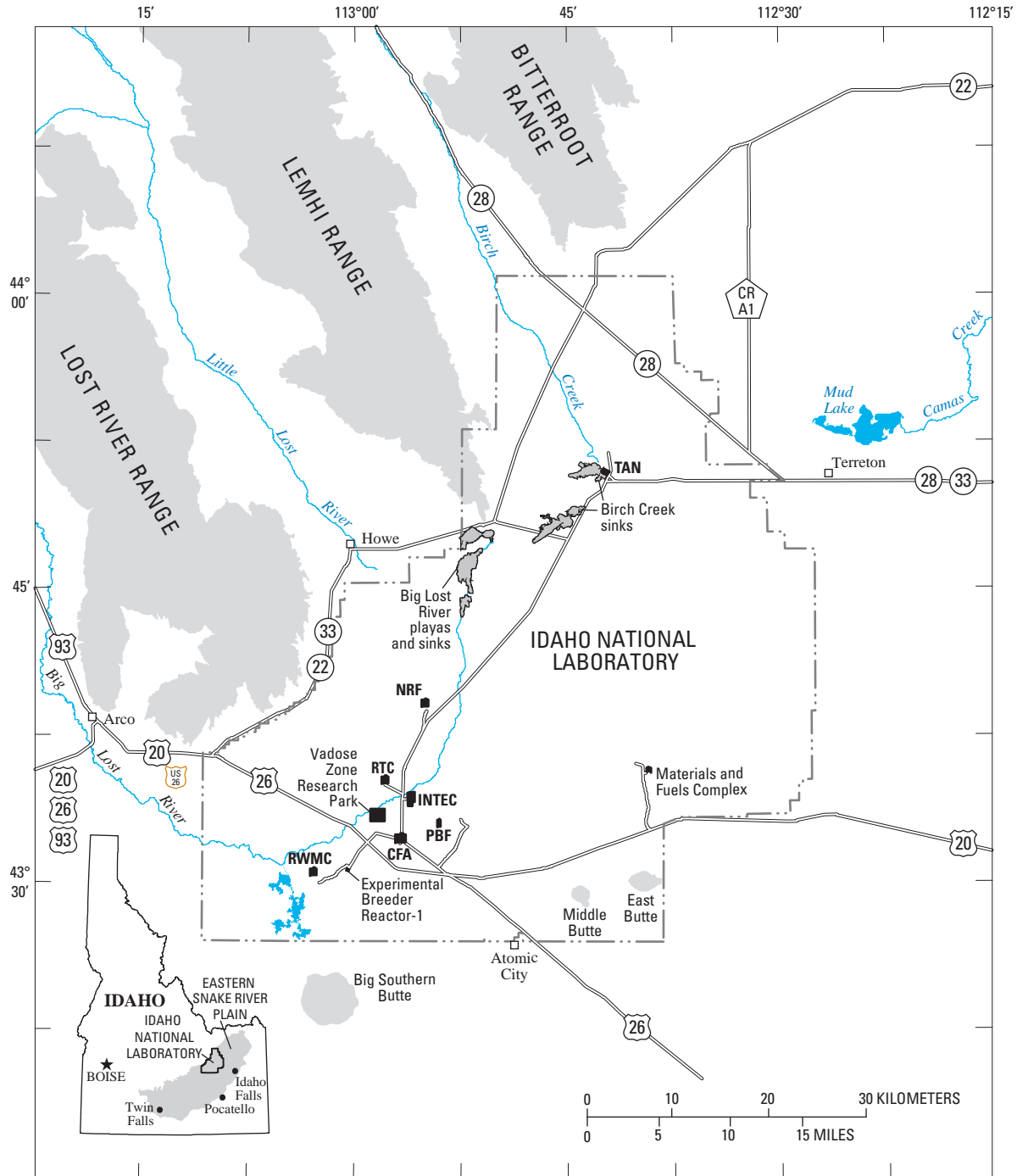
The degree to which the unsaturated hydraulic conductivity curves estimated from property-transfer-modeled water-retention parameters and saturated hydraulic conductivity approximated the laboratory-measured data was evaluated using a goodness-of-fit indicator, the root-mean-square error. Because numerical models of variably saturated flow and transport require parameterized hydraulic properties as input, simulations were run to evaluate the effect of the various parameters on model results. Results show that the property transfer models based on easily measured bulk properties perform nearly as well as using curve fits to laboratory-measured water retention for the estimation of unsaturated hydraulic conductivity.

## Introduction

The unsaturated zone at the Idaho National Laboratory (INL) consists of thick layers of fractured basalt interbedded with thin layers of fluvial, eolian, and lacustrine sediments. These sedimentary interbeds affect both vertical and horizontal flow through the unsaturated zone although the processes are not well understood. The sedimentary interbeds may affect the flow in several ways, including the retardation of downward-moving water as the water encounters layer boundaries; the generation of perched water; the homogenization of flow that has been focused by basalt fractures; and the formation of long-range, highly conductive horizontal flow paths for contaminants. To better understand the flow processes, the role of the sedimentary interbeds needs to be determined; this determination typically is accomplished using numerical flow model simulations. Numerical flow models require input of two basic unsaturated hydraulic properties—water-retention [ $\theta(\psi)$ , defined as water content ( $\theta$ ) as a function of matric pressure ( $\psi$ )] and unsaturated hydraulic conductivity [ $K(\theta)$ , defined as hydraulic conductivity ( $K$ ) as a function of water content ( $\theta$ )].

Because laboratory measurement of  $\theta(\psi)$  and  $K(\theta)$  requires special equipment and expertise and may require weeks to complete for a single core sample and because of the thick (as much as 200 m) unsaturated zone at the INL ([fig. 1](#)) and the complex stratigraphy and large site area, core-sample data are available for only a small fraction of the subsurface sediments. However, particle-size distribution and other bulk property data are available because, when core samples were not obtained during drilling, borehole cuttings often were collected for particle-size analysis. These particle-size distribution and other bulk physical-property data can be used in property-transfer models (PTMs) developed by Winfield (2005) to predict  $\theta(\psi)$ , thereby reducing the need for laboratory measurement of unsaturated hydraulic properties. The bulk physical-property data used in the PTMs includes bulk density ( $\rho_{bulk}$ ) and the uniformity coefficient ( $C_u$ ) and median particle diameter ( $d_{50}$ ) derived from particle-size analysis.

## 2 Property-Transfer Modeling to Estimate Unsaturated Hydraulic Conductivity of Deep Sediments, INL, Idaho



Base from U.S. Geological Survey, 1:100,000, Arco quadrangle, 1989, Blackfoot quadrangle, 1997, Borah Peak quadrangle, 1989, Circular Butte quadrangle, 1980, Craters of the Moon quadrangle, 1978, and Dubois quadrangle, 1983, digital data, 1:24,000 and 1:100,000

### EXPLANATION

□	<b>Selected facilities at the Idaho National Laboratory</b>	RWMC	Radioactive Waste Management Complex
CFA	Central Facilities Area	RTC	Reactor Technology Complex
INTEC	Idaho Nuclear Technology and Engineering Center	TAN	Test Area North
NRF	Naval Reactors Facility	---	<b>Boundary of Idaho National Laboratory</b>
PBF	Power Burst Facility		

**Figure 1.** Locations of the Idaho National Laboratory, Idaho, and selected facilities.

Because  $\theta(\psi)$  and  $K(\theta)$  vary nonlinearly, parametric models commonly are used to represent the curves for those properties. The Rossi-Nimmo (1994) junction (RNJ) model, which was used in the development of the PTMs by Winfield (2005), requires three parameters to describe the entire range of  $\psi$ ; therefore, three separate multiple linear-regression equations were developed. These multiple linear-regression equations were used by Winfield (2005) to develop two separate PTMs, one for  $\theta(\psi)$  and the other for saturated hydraulic conductivity ( $K_{sat}$ ) (Winfield, 2005). This study combines the PTMs developed by Winfield (2005) and the capillary-bundle model developed by Mualem (1976) to estimate  $K(\theta)$ .

## Site Description

The INL was established in 1949 under the U.S. Atomic Energy Commission, now the U.S. Department of Energy, for nuclear energy research. The INL occupies about 2,300 km<sup>2</sup> of the west-central part of the eastern Snake River Plain (SRP). The site hosts several facilities (fig. 1) of which at least four have been used to generate, store, or dispose of radioactive, organic, and inorganic wastes. These facilities include the (1) Radioactive Waste Management Complex (RWMC); (2) Idaho Nuclear Technology and Engineering Center (INTEC); formerly known as the Idaho Chemical Processing Plant (ICPP); (3) Reactor Technology Complex (RTC), formerly known as the Test Reactor Area (TRA); and (4) Test Area North (TAN).

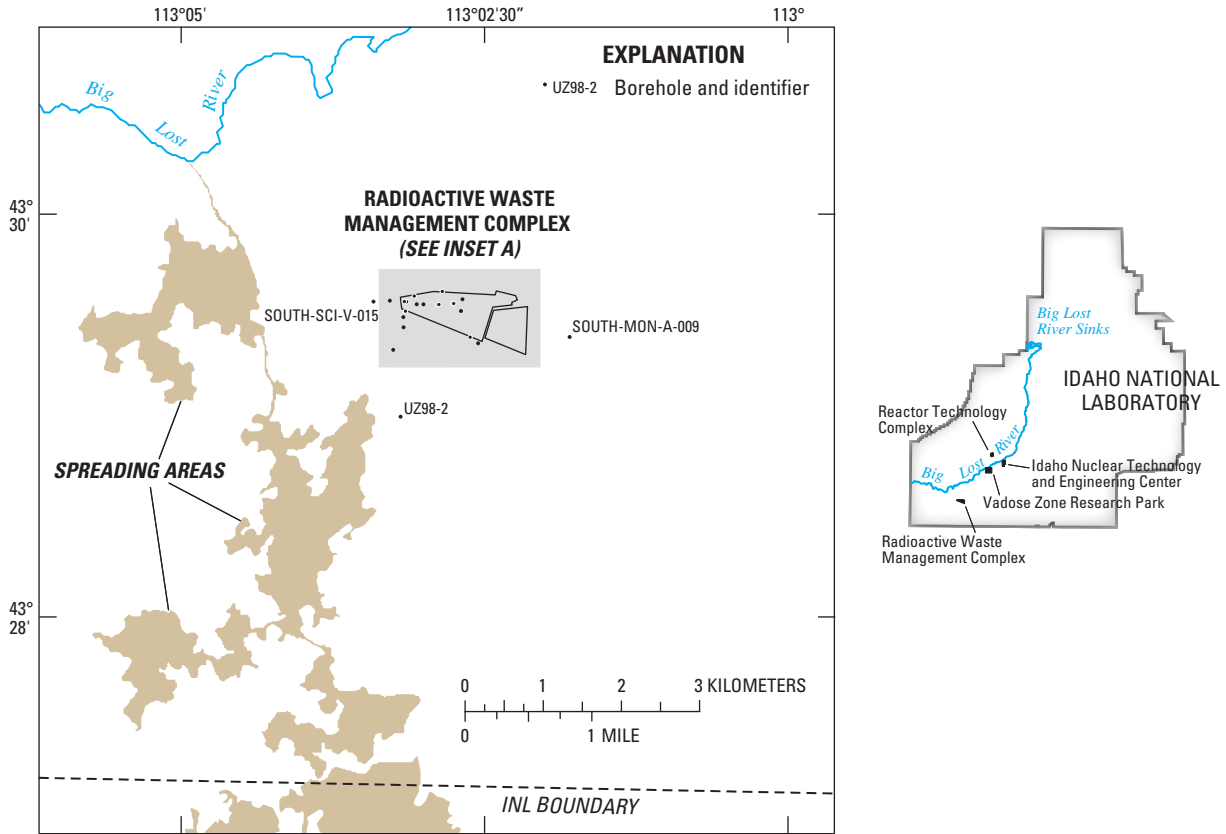
The eastern SRP is a northeast-trending basin, approximately 320 km long and 80 to 110 km wide, that slopes gently to the southwest and is bordered by northwest-trending mountain ranges. The eastern SRP is underlain by interbedded volcanic and sedimentary layers that extend as much as 3,000 m below land surface. The sedimentary interbeds result from quiet intervals between volcanic eruptions and are of fluvial, eolian, and lacustrine origin with large amounts of sand, silt, and clay. Volcanic units, composed primarily of basalt flows, welded ash flows, and rhyolite, may be vesicular to massive with either horizontal or vertical fracture patterns. Near the INTEC, boreholes drilled to 200-m depths penetrate a sequence of 23 basalt-flow groups and 15 to 20 sedimentary interbeds (Anderson, 1991). The surficial sediments near the INTEC consist of gravelly alluvium, range from 2 to 20 m thick, and are thickest to the northwest (Anderson and others, 1996). Beneath the RWMC, 10 basalt-flow groups and 7 major sedimentary interbeds have been identified from boreholes drilled up to 220-m depth. Surficial sediments at the RWMC are composed primarily of silt and clay and range from 0 to 7 m thick (Rightmire and Lewis, 1987; Anderson and Lewis, 1989).

The climate of the eastern SRP is semiarid and the average annual precipitation is 22 cm. Parts of the SRP aquifer underlie the INL. The depth to the water table ranges from 60 m in the northern part of the INL to about 200 m in the southern part (Barraclough and others, 1981; Liszewski and Mann, 1992). The depth to the water table is about 145 m below the INTEC and about 180 m below the RWMC. The predominant direction of ground-water flow is from northeast to southwest. Recharge to the aquifer is primarily from irrigation water diversions from streams, precipitation and snowmelt, underflow from tributary-valley streams, and seepage from surface-water bodies (Hackett and others, 1986). Within the INL boundaries, the Big Lost River (fig. 1) is an intermittent stream that flows from southwest to northeast about 3 km north of the RWMC (fig. 2) and less than 1 km north of the INTEC (fig. 3). Because of the proximity of the Big Lost River to waste-disposal and storage facilities, a diversion dam was constructed in 1958 to reduce the threat of flooding (Barraclough and others, 1967). During high-flow periods, flow is diverted to topographic depressions (referred to as spreading areas) less than 2 km west of the RWMC (fig. 2).

## Previous Investigations

Because of the site's history of chemical-waste production and the potential for radionuclide migration from the shallow subsurface to the SRP aquifer, the role of the thick unsaturated zone in contaminant transport processes needs to be investigated. Few studies have been done in which hydraulic properties of deep unsaturated-zone sediments at the INL have been determined from core samples. Only two locations within the INL have been characterized, the RWMC (fig. 2) and the Vadose Zone Research Park (VZRP) near the INTEC (fig. 3). McElroy and Hubbell (1990) presented  $\theta(\psi)$ , particle size, and  $\rho_{bulk}$  data measured on sedimentary interbed core samples collected from eight boreholes near the RWMC.  $\theta(\psi)$ ,  $K(\theta)$ , and bulk-physical property data from core-sample measurements were presented by Perkins and Nimmo (2000) for one borehole about 1.5 km southwest of the SDA (fig. 2). Measurements from an additional 16 boreholes also have been completed on sediment core samples collected from near the SDA (S. O. Magnuson, Battelle Energy Alliance, written commun., 2002). Perkins (2003) and Winfield (2003) presented unsaturated hydraulic- and bulk physical-property measurements for seven boreholes near the current percolation pond area for the INTEC facility at the VZRP (fig. 3).

4 Property-Transfer Modeling to Estimate Unsaturated Hydraulic Conductivity of Deep Sediments, INL, Idaho



Base from U.S. Geological Survey, 1:24,000, Arco Hills SE quadrangle, 1972, and Big Southern Butte quadrangle, 1972

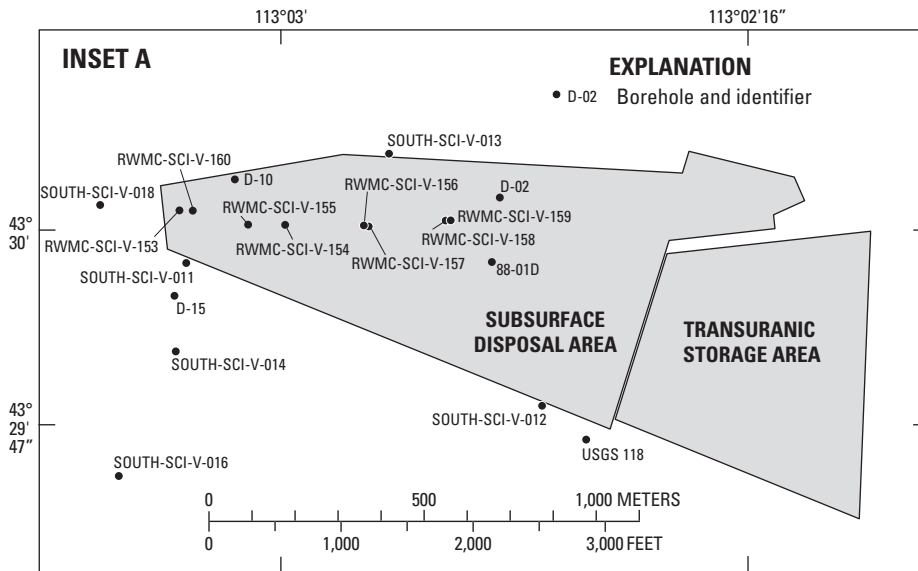


**Figure 2.** Locations of boreholes in the Radioactive Waste Management Complex, Idaho National Laboratory, Idaho, from which sedimentary interbed core samples were used to develop property-transfer models.

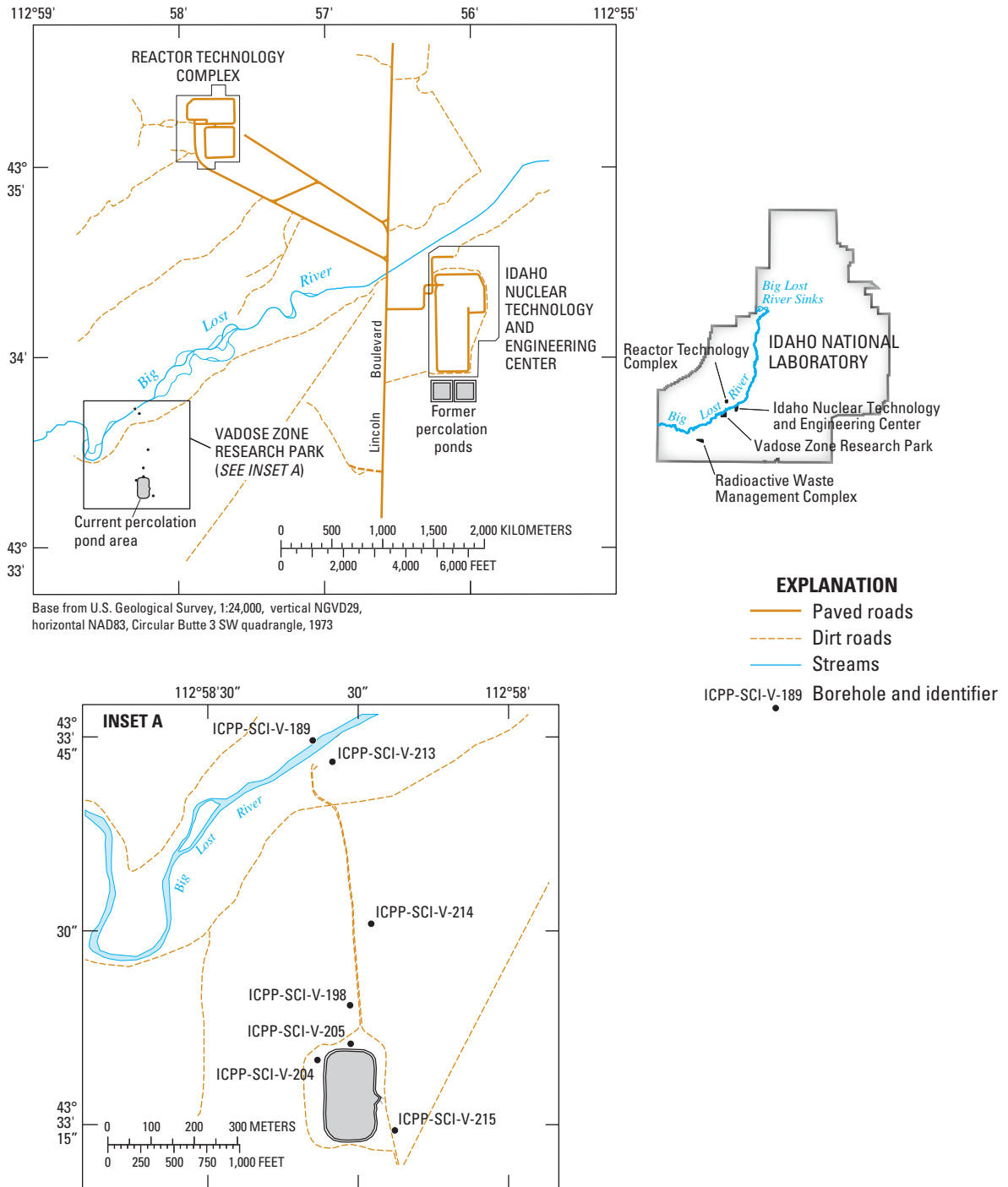


**Figure 3.** Locations of boreholes in the Vadose Zone Research Park, Idaho National Laboratory, Idaho, from which sedimentary interbed core samples were used to develop property-transfer models.

## Purpose and Scope

Development of a PTM to estimate  $K(\theta)$  is important for regional unsaturated-flow models where data do not exist for every point in space. This report describes the combination of Mualem's (1976) capillary-bundle model for estimating  $K(\theta)$  and the site-specific PTMs developed by Winfield (2005) for predicting  $\theta(\psi)$  and  $K_{sat}$  of the sedimentary interbeds underlying the INL. The Winfield (2005) PTMs were developed using available data for two locations within the INL, the RWMC (fig. 2) and the VZRP (fig. 3). Multiple linear-regression equations were used to estimate hydraulic properties from bulk-physical property data compiled from previous studies for 109 core samples (Winfield, 2005). Regression equations were developed for hydraulic parameters defining the  $\theta(\psi)$  curve [saturated water content ( $\theta_{sat}$ ) and two parameters from the RNJ model] and  $K_{sat}$ . Winfield (2005) described the available data, data selection and processing, multiple linear-regression assumptions and approach, and regression equations developed for each parameter. The extension of the Winfield (2005) PTMs for estimating  $K(\theta)$  in this study includes a subset of data for 40 samples, which are the only samples for which laboratory-measured  $K(\theta)$  data from minimally disturbed core samples are available (Perkins and Nimmo, 2000; Perkins, 2003; Winfield, 2003).

This report presents a procedure for using the PTMs developed by Winfield (2005) for estimating  $K(\theta)$ .  $K(\theta)$  curves estimated from PTM-estimated  $\theta(\psi)$  and  $K_{sat}$  combined with Mualem's (1976) capillary-bundle model are compared to those (1) obtained with data measured directly in the laboratory, (2) estimated on the basis of RNJ fits to measured water retention, and (3) estimated on the basis of van Genuchten (1980) fits (referred to as vG curve fits) to measured water retention. Illustrative numerical simulations are presented to provide information on the performance of the PTMs in predicting unsaturated flow dynamics.

## Hydraulic Conductivity Estimation Approach

To estimate  $K(\theta)$  for the sedimentary interbeds underlying the INL,  $\theta(\psi)$  and  $K_{sat}$  parameters were combined with Mualem's (1976) capillary-bundle model, one of the most widely used  $K(\theta)$  models available. Mualem's model infers a pore-size distribution for a soil from its  $\theta(\psi)$  curve based on capillary theory, which assumes that a pore radius is proportional to the  $\psi$  value at which that pore drains. Mualem's model conceptualizes pores as pairs of capillary tubes whose lengths are proportional to their radii; the

conductance of each capillary-tube pair is determined according to Poiseuille's law<sup>1</sup>. In this formulation,  $K(\theta)$  is defined as

$$K(\theta) = K_r(\theta)K_{sat}, \quad (1)$$

where

$K_r(\theta)$  is relative hydraulic conductivity.

To compute  $K(\theta)$  for the whole medium, the conductance of all capillary-tube pairs is integrated as

$$K_r(\theta) = S_e^L \left[ \frac{\int_0^\theta \frac{1}{\psi(\theta)} d\theta}{\int_0^{\theta_{sat}} \frac{1}{\psi(\theta)} d\theta} \right]^2, \quad (2)$$

where

$$S_e = \frac{\theta - \theta_r}{\theta_{sat} - \theta_r},$$

$\theta_r$  is residual water content expressed volumetrically,

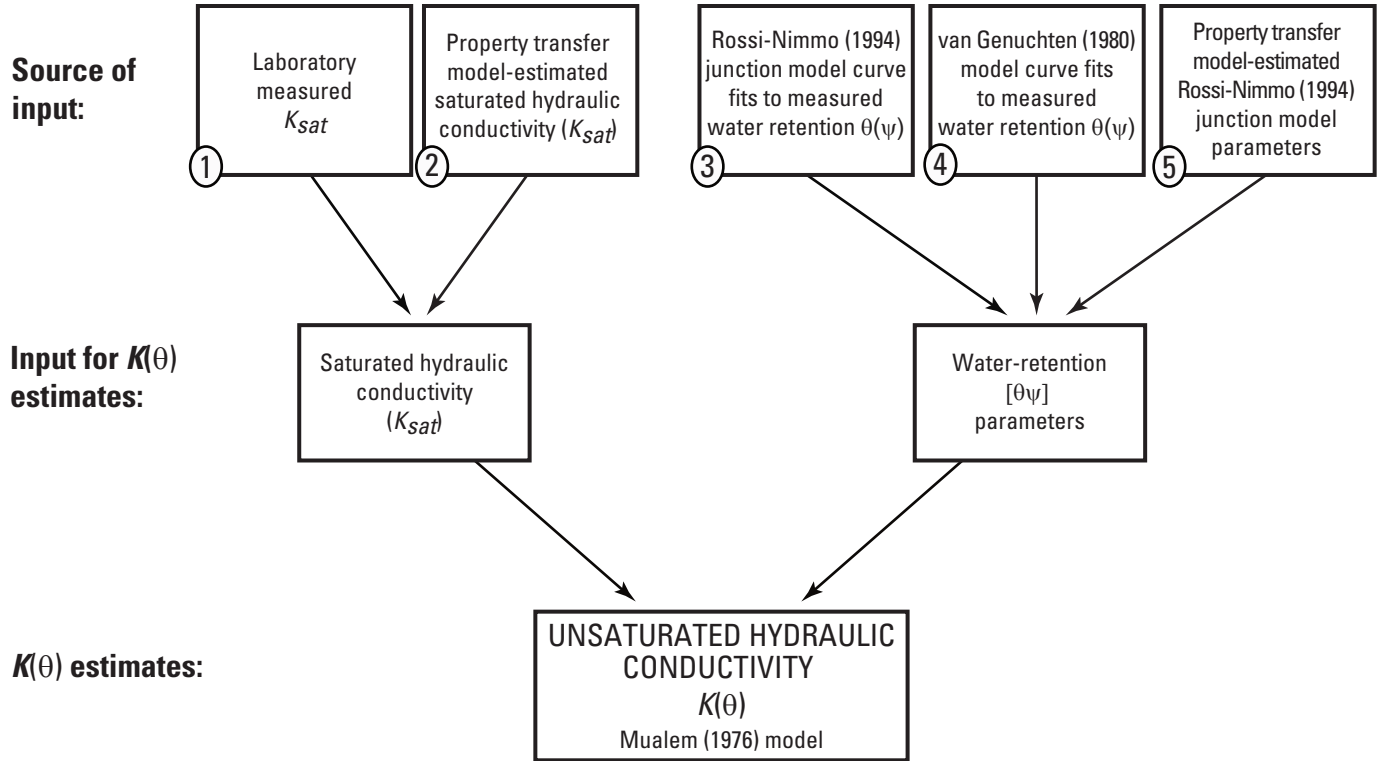
$\theta_{sat}$  is saturated water content expressed volumetrically,

$L$  is a dimensionless parameter interpreted as representing the tortuosity and connectivity of pores with different sizes and usually is given the value of 0.5, and

$\psi(\theta)$  is the retention curve with matric pressure expressed as a function of water content.

Laboratory-measured  $K(\theta)$  values were compared to those estimated by equation 1 using four model variations: (1) PTM-estimated  $K_{sat}$  and RNJ model parameters (referred to as the RNJ-PTM- $K_{sat}$  model), (2) laboratory-measured  $K_{sat}$  and PTM-estimated RNJ model parameters (referred to as the RNJ-PTM model), (3) laboratory-measured  $K_{sat}$  and RNJ model curve fits to measured water retention (referred to as the RNJ-CF model), and (4) laboratory-measured  $K_{sat}$  and vG model curve fits to measured water retention (referred to as the vG-CF model). The basic steps for estimating  $K(\theta)$  are outlined in [figure 4](#) and [table 1](#).

<sup>1</sup> Poiseuille's law states that the flow rate per unit cross-sectional area of a capillary tube is proportional to the square of the radius.



**Model variations evaluated:**

- 1 and 3 (referred to as the RNJ-CF model)
- 1 and 4 (referred to as the vG-CF model)
- 1 and 5 (referred to as the RNJ-PTM model)
- 2 and 5 (referred to as the RNJ-PTM- $K_{sat}$  model)

**Figure 4.** Steps used to estimate unsaturated hydraulic conductivity.

**Table 1.** Model variations used to estimate unsaturated hydraulic conductivity.

[Abbreviations: RNJ-PTM- $K_{sat}$ , property-transfer model-estimated saturated hydraulic conductivity and Rossi-Nimmo junction model parameters; RNJ-PTM, laboratory-measured saturated hydraulic conductivity and property-transfer model-estimated Rossi-Nimmo junction model parameters; RNJ-CF, laboratory-measured saturated hydraulic conductivity and Rossi-Nimmo junction model curve fits to measured water retention; vG-CF, laboratory-measured saturated hydraulic conductivity and van Genuchten model curve fits to measured water retention]

Source of input	Laboratory-measured $K_{sat}$	Property-transfer model-estimated saturated hydraulic conductivity ( $K_{sat}$ )	Model curve fits to measured water retention $\theta(\psi)$		Property-transfer model-estimated Rossi-Nimmo junction model parameters
			Rossi-Nimmo junction	van Genuchten	
RNJ-PTM- $K_{sat}$ model		X			X
RNJ-PTM model	X				X
RNJ-CF model	X		X		
vG-CF model	X			X	

**Data Sets**

A subset of the data for the core samples used by Winfield (2005) to develop PTMs for  $\theta(\psi)$  and  $K_{sat}$  was used to estimate  $K(\theta)$ . The 40 minimally disturbed core samples (table 2) used in this study were chosen because they are the only samples for which  $\theta(\psi)$  and  $K(\theta)$  were measured directly in the laboratory. The laboratory-measured  $\theta(\psi)$  and  $K(\theta)$  values for these deep core samples, in addition to bulk physical-property data, are presented by Perkins and Nimmo (2000) for borehole UZ98-2, about 1.5 km southwest of

the RWMC subsurface disposal area (SDA) (fig. 2), and by Perkins (2003) and Winfield (2003) for seven boreholes near the current percolation pond area for the INTEC facility at the VZRP (fig. 3). The U.S. Department of Agriculture’s (USDA) textural classifications (Soil Survey Staff, 1975) for all core samples used in this study are presented in figure 5. Materials with high clay and gravel content known to exist within the sedimentary interbeds underlying the INL are under-represented in this subset.

**Table 2.** Core samples used to estimate unsaturated hydraulic conductivity in sedimentary interbeds underlying the Idaho National Laboratory, Idaho.

[Abbreviations: RWMC, Radioactive Waste Management Complex; VZRP, Vadose Zone Research Park]

Borehole identification	Borehole location	Depth interval (meter)	Number of core samples	Study
UZ98-2	RWMC	42.98–50.30	18	Perkins and Nimmo (2000)
ICPP-SCI-V-215	VZRP	45.54–59.92	12	Perkins (2003)
ICPP-SCI-V-189, ICPP-SCI-V-198, ICPP-SCI-V-204, ICPP-SCI-V-205, ICPP-SCI-V-213, ICPP-SCI-V-214	VZRP	36.59–56.33	10	Winfield (2003)
Total number of samples			40	

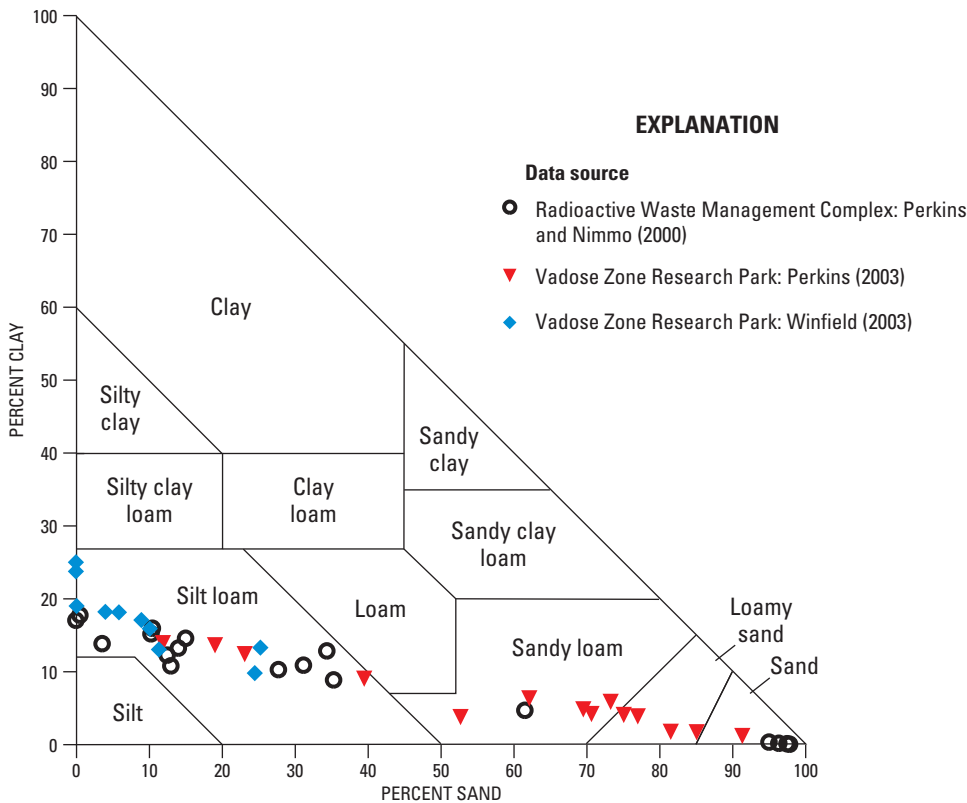


**Figure 5.** Textural classification of core samples (based on the system of the U.S. Department of Agriculture [Soil Survey Staff, 1975]) used to evaluate property-transfer model for estimating unsaturated hydraulic conductivity  $K(\theta)$ .



### Water-Retention Parameters and Hydraulic Conductivity Estimation

In the development of the PTMs by Winfield (2005), the RNJ model was used to fit laboratory-measured  $\theta(\psi)$  values. The RNJ model is more physically realistic for the entire range of  $\theta$  from saturation to oven dryness ( $\psi_d$ ) than other parametric models (for example, Brooks and Corey, 1964, and van Genuchten, 1980) that include the empirical, optimized residual water content ( $\theta_r$ ) parameter, which is not well defined. According to capillary theory the largest pores, associated with  $\psi$  values near zero, drain first. Drainage of those pores is followed by drainage of successively smaller pores as  $\theta$  approaches  $\theta_r$ . The Brooks and Corey and van Genuchten models have an asymptotic approach to  $\theta_r$ , meaning that the number of small pores approaches infinity, which is physically unrealistic. The  $\theta(\psi)$  curve represented by the RNJ model does not have a parameter analogous to  $\theta_r$ ; the curve goes to zero  $\theta$  at a fixed  $\psi$  value calculated for the conditions of  $\psi_d$ . The RNJ model, like many other parametric water-retention models, can be combined analytically with the capillary-bundle model developed by Mualem (1976) to estimate  $K(\theta)$  (Fayer and others, 1992; Rossi and Nimmo, 1994; Andraski, 1996; Andraski and Jacobson, 2000).

The RNJ model consists of three functions joined at two points (defined as  $\psi_i$  and  $\psi_j$ , fig. 6). These functions are a parabolic function for the wet range of  $\psi$  ( $\psi_i \leq \psi \leq 0$ ), a power-law function (Brooks and Corey, 1964) for the middle range of  $\psi$  ( $\psi_j \leq \psi \leq \psi_i$ ), and a logarithmic function for the dry range of  $\psi$  ( $\psi_d \leq \psi \leq \psi_j$ ). The model has two independent parameters: (1) the scaling factor for  $\psi$  ( $\psi_o$ ), and (2) the curve-shape parameter ( $\lambda$ ). Sometimes,  $\psi_o$  is associated with the  $\psi$  value at which air first enters a porous material during desaturation (referred to as air-entry pressure). In actuality, however, air begins displacing water in the largest pores at a higher (less negative)  $\psi$  than  $\psi_o$ , as evidenced by the departure of  $\theta$  from saturation to the right of  $\psi_o$  on the  $\theta(\psi)$  curve (fig. 6). Unlike the model of Brooks and Corey, which holds  $\theta$  fixed between  $\psi = 0$  and the air-entry pressure, the RNJ model produces a smooth curve near saturation, represented by a parabolic function, that allows the pore-size distribution [the first derivative of the  $\theta(\psi)$  curve] to be represented more realistically. The curve-shape parameter  $\lambda$  indicates the relative steepness of the middle part of the  $\theta(\psi)$  curve, described by the power-law function. Larger  $\lambda$  values cause the drainage part of the  $\theta(\psi)$  curve to appear steeper.

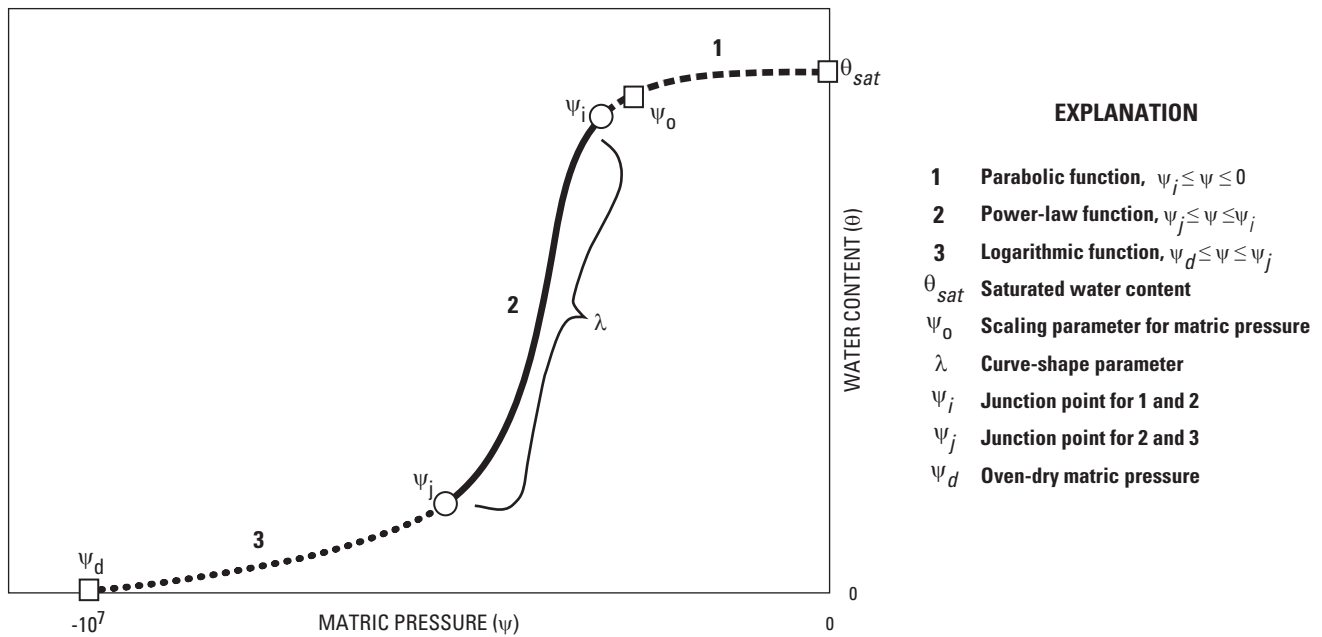


**Figure 6.** Example of water-retention [ $\theta(\psi)$ ] curve showing components of the curve-fit model developed by Rossi and Nimmo (1994).

## 10 Property-Transfer Modeling to Estimate Unsaturated Hydraulic Conductivity of Deep Sediments, INL, Idaho

The parabolic function applies for  $\psi_i \leq \psi \leq 0$  and is represented by

$$\frac{\theta}{\theta_{sat}} = 1 - c \left( \frac{\psi}{\psi_o} \right)^2, \quad (3)$$

where

$c$  is a dimensionless constant calculated from an analytical function involving the parameter  $\lambda$  (described below), which also is dimensionless.

The power-law function applies for  $\psi_j \leq \psi \leq \psi_i$  and is represented by

$$\frac{\theta}{\theta_{sat}} = \left( \frac{\psi_o}{\psi} \right)^\lambda. \quad (4)$$

The logarithmic function applies for  $\psi_d \leq \psi \leq \psi_j$  and is represented by

$$\frac{\theta}{\theta_{sat}} = \alpha \ln \left( \frac{\psi_d}{\psi} \right). \quad (5)$$

The dependent parameters are calculated as follows:

$$\begin{aligned} \alpha &= \lambda e \left( \frac{\psi_o}{\psi_d} \right)^\lambda, \\ \psi_i &= \psi_o \left( \frac{2}{2+\lambda} \right)^{\frac{-1}{\lambda}}, \\ \psi_j &= \psi_d e^{\frac{-1}{\lambda}}, \text{ and} \\ c &= 0.5\lambda \left( \frac{2}{2+\lambda} \right)^{\frac{\lambda+2}{\lambda}}. \end{aligned} \quad (6)$$

For convenience, a  $\psi_d$  value of  $-1 \times 10^7$  cm-water (the pressure at which the curve goes to zero  $\theta$ ) was used in the model fits for all core samples. That value is considered reasonable for a soil dried in an oven at 105–110°C with 50-percent relative humidity (Ross and others, 1991; Rossi and Nimmo, 1994).

Winfield (2005) formulated the following property-transfer equations for the RNJ model parameters and  $K_{sat}$  using particle-size statistics [median particle diameter ( $d_{50}$ ) and uniformity coefficient ( $C_u$ )] and  $\rho_{bulk}$  as input

$$\begin{aligned} \theta_{sat} &= 1.0063 - 0.3998\rho_{bulk} - 0.0123\log(d_{50}) - 0.0029\log(C_u), \\ \log(\psi_o) &= -1.4080 + 1.5344\rho_{bulk} - 0.8394\log(d_{50}) - 0.1510\log(C_u), \\ \text{and} \\ \log(\lambda) &= -0.0411 + 0.0974\rho_{bulk} + 0.1925\log(d_{50}) - 0.4910\log(C_u). \end{aligned} \quad (7)$$

The  $K_{sat}$  model equation is

$$\begin{aligned} \log(K_{sat}) &= -1.7690 + 0.0794\rho_{bulk} \\ &+ 1.7507\log(d_{50}) - 0.3274\log(C_u). \end{aligned} \quad (8)$$

The RNJ model is integrable in closed form for use in the Mualem (1976) model (Rossi and Nimmo, 1994). In the Mualem model,  $K_r(\theta)$ , the ratio between the unsaturated and saturated hydraulic conductivity can be expressed as

$$K_r(\theta) = \sqrt{\frac{\theta}{\theta_{sat}}} \frac{I^2(\theta)}{I^2(\theta_{sat})}, \quad (9)$$

where

$$\begin{aligned} I(\theta) &= I_{\text{III}}(\theta) \text{ for } \theta \leq \theta_j, \\ I(\theta) &= I_{\text{II}}(\theta) \text{ for } \theta_j \leq \theta \leq \theta_i, \text{ and} \\ I(\theta) &= I_{\text{I}}(\theta) \text{ for } \theta_i \leq \theta \leq \theta_{sat}, \end{aligned} \quad (10)$$

and

$$\begin{aligned} I_{\text{III}}(\theta) &= \frac{\alpha}{\psi_d} \left[ \exp \left( \frac{1}{\alpha} \frac{\theta}{\theta_{sat}} \right) - 1 \right], \\ I_{\text{II}}(\theta) &= I_{\text{III}}(\theta_j) + \frac{1}{\psi_o} \frac{\lambda}{\lambda+1} \left[ \left( \frac{\theta}{\theta_{sat}} \right)^{\frac{(\lambda+1)}{\lambda}} - \left( \frac{\theta_j}{\theta_{sat}} \right)^{\frac{(\lambda+1)}{\lambda}} \right], \\ \text{and} \\ I_{\text{I}}(\theta) &= I_{\text{II}}(\theta_i) + \frac{2c^{1/2}}{\psi_o} \left[ \left( 1 - \frac{\theta_i}{\theta_{sat}} \right)^{1/2} - \left( 1 - \frac{\theta}{\theta_{sat}} \right)^{1/2} \right], \\ \theta_j &= \theta(\psi_j) \quad \theta_i = \theta(\psi_i). \end{aligned} \quad (11)$$

For comparison purposes, the measured  $\theta(\psi)$  data also were fit with the empirical formula of van Genuchten (1980), which has the form

$$\theta(\psi) = \theta_r + \left\{ (\theta_{sat} - \theta_r) / \left[ 1 + (\alpha\psi)^n \right]^m \right\}, \quad (12)$$

where  $\alpha$ ,  $n$ , and  $m$  are empirical, dimensionless fitting parameters.

Using measured  $\theta$  and  $\psi$  values,  $\alpha$  and  $n$  parameters are optimized to achieve the best fit to the data. The parameter  $m$  is set equal to  $1-1/n$  to reduce the number of independent parameters and, thus, allow for better model convergence and to permit convenient mathematical combination with Mualem's (1976) model (van Genuchten, 1980) as follows

$$K(\theta) = K_{sat} S_e^L \{ 1 - [1 - S_e^{n/(n-1)}]^{1-(1/n)} \}^2. \quad (13)$$

Most widely used unsaturated flow and transport models use the van Genuchten (1980) model rather than the RNJ model to represent  $\theta(\psi)$ . The van Genuchten (1980) equation is parameterized by  $\theta_{sat}$ ,  $\theta_r$ ,  $\alpha$ , and  $n$ , where the scaling parameter for  $\psi$  is  $\alpha$  (analogous to  $\psi_o$ ) and the curve-shape parameter is  $n$  (analogous to  $\lambda$ ).

## Results and Discussion

The results from the four model variations presented in this report were evaluated in two ways to assess model performance. Root-mean-square error values were calculated as described later to directly quantify the difference between laboratory-measured and model-estimated  $K(\theta)$  data points. Because unsaturated hydraulic property parameters are necessary input in predictive modeling of variably saturated flow and transport, a numerical computer model for simulating unsaturated ground-water flow was used to illustrate the effect of parameter variation on model results.

### Root-Mean-Square Error Analysis

The root-mean-square error (RMSE), also referred to as the standard error of the estimate, is used in this study as a goodness-of-fit indicator between measured and estimated  $K(\theta)$  values. The RMSE is calculated as

$$RMSE = \sqrt{\frac{\sum_{j=1}^n (y_j - \hat{y}_j)^2}{n}}, \quad (14)$$

where

- $y_j$  is the measured value,
- $\hat{y}_j$  is the estimated value of the dependent variable and,
- $n$  is the number of observations.

Small RMSE values indicate the estimated value is closer to the measured value of the variable.  $K(\theta)$  values span several orders of magnitude, thus, in effect, unequally weighting points in the RMSE calculation. Therefore, the  $K(\theta)$  values were transformed logarithmically prior to calculation. The number of  $K(\theta)$  points ( $n$ ) measured for each sample was between 3 and 10. Ranges in the number of measured points and the average number of measured points for the samples from each data set are given in [table 3](#).

**Table 3.** Ranges in number of measured unsaturated hydraulic conductivity points and average number of measured points for samples from three data sets used in the root-mean-square error analysis.

[Abbreviations:  $K(\theta)$ , unsaturated hydraulic conductivity]

Study	Range in number of measured $K(\theta)$ points	Average number of measured $K(\theta)$ points
Perkins and Nimmo (2000)	3–10	6
Perkins (2003)	4–8	7
Winfield (2003)	3–8	5

To illustrate the performance of the four models (RNJ-PTM- $K_{sat}$ , RNJ-PTM, RNJ-CF, and vG-CF),  $K(\theta)$  curves are shown in [figures 7–10](#) along with laboratory-measured data points for four samples from each of the three data sets used in this study. RMSE values were calculated for the 40 minimally disturbed core samples using the difference between laboratory-measured and estimated  $K(\theta)$  points to quantify goodness of fit. RMSE values in terms of  $\log K(\theta)$  ranged from 0.30 to 3.28 and had an average of 1.15 for the RNJ-PTM- $K_{sat}$  model, ranged from 0.28 to 2.97 and had an average of 1.05 for the RNJ-PTM model, ranged from 0.21 to 2.19 and had an average of 0.85 for the RNJ-CF model, and ranged from 0.35 to 9.45 and had an average of 1.61 for the vG-CF model. For 35 percent of the samples,  $K(\theta)$  was best estimated by one of the property-transfer models (either the RNJ-PTM- $K_{sat}$  or the RNJ-PTM model). For another 35 percent, the RNJ-CF model was best, and for the remaining 30 percent, the vG-CF model was best. For 25 of the 40 core samples,  $K(\theta)$  was better estimated by the RNJ-CF model than the vG-CF model.

The statistical distributions of RMSE values are shown in [figure 11](#). The distributions indicate that the differences between the RNJ-PTM- $K_{sat}$  and RNJ-PTM models are small and that using a laboratory-measured  $K_{sat}$  value only slightly improves the  $K(\theta)$  estimates. The lack of correlation between  $K(\theta)$  values estimated from PTMs in terms of the root-mean-square error and  $K_{sat}$  values in terms of the difference between the measured and estimated values is shown in [figure 12](#).

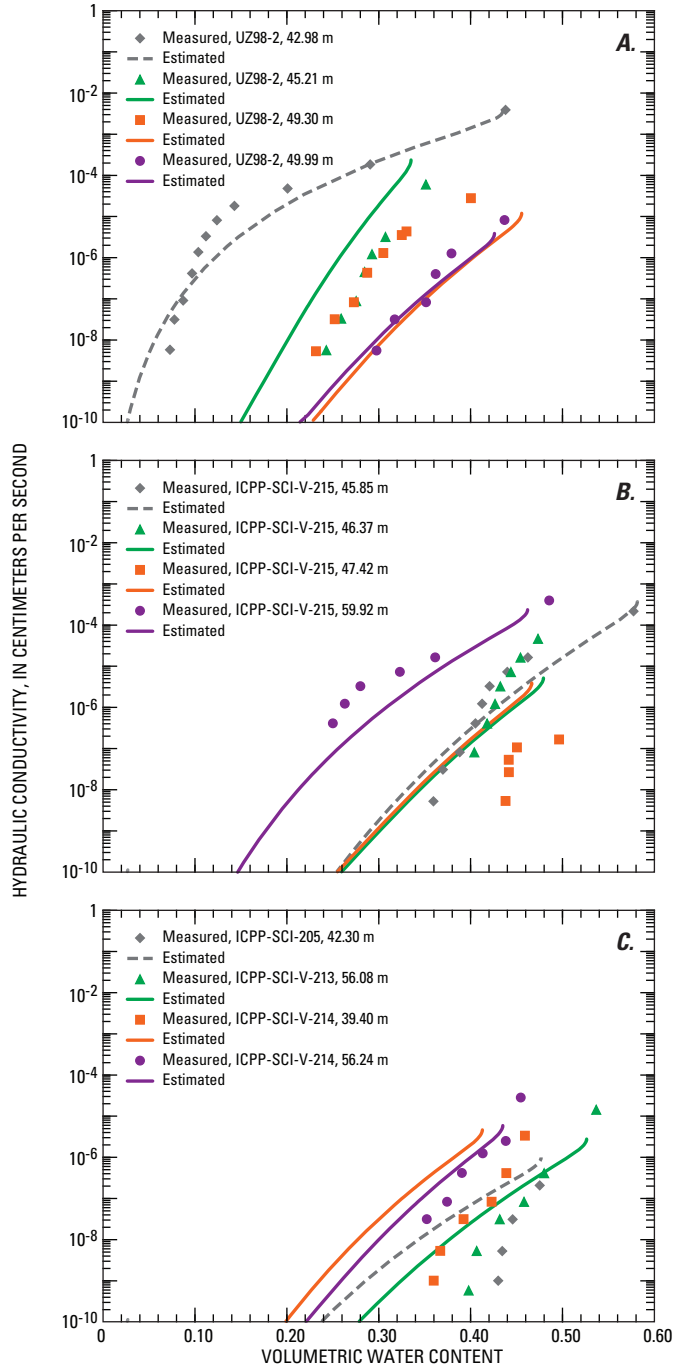


**Figure 7.** Unsaturated hydraulic conductivity curves estimated using the RNJ-PTM- $K_{sat}$  model (property-transfer model-estimated saturated hydraulic conductivity and Rossi-Nimmo junction model parameters). Graphs A, B, and C show four samples each from Perkins and Nimmo (2000), Perkins (2003), and Winfield (2003), respectively.

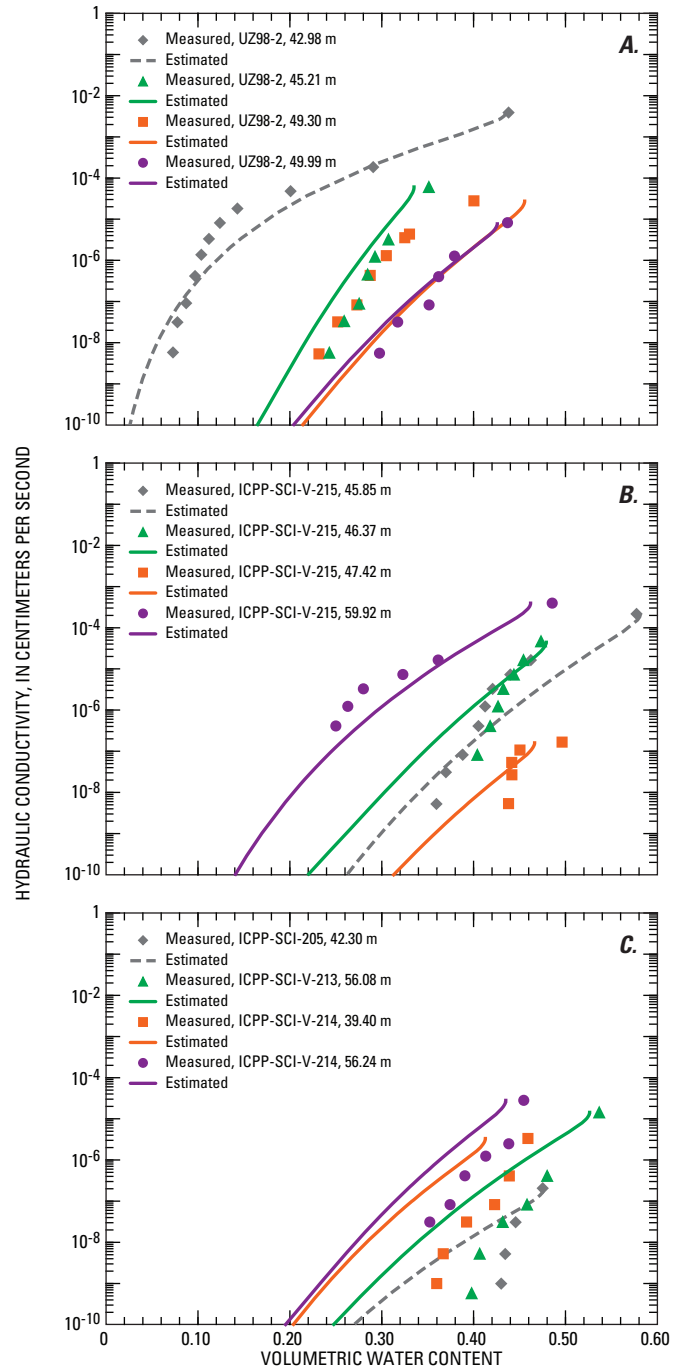


**Figure 8.** Unsaturated hydraulic conductivity curves estimated using the RNJ-PTM model (laboratory-measured saturated hydraulic conductivity and property-transfer model-estimated Rossi-Nimmo junction model parameters). Graphs A, B, and C show four samples each from Perkins and Nimmo (2000), Perkins (2003), and Winfield (2003), respectively.

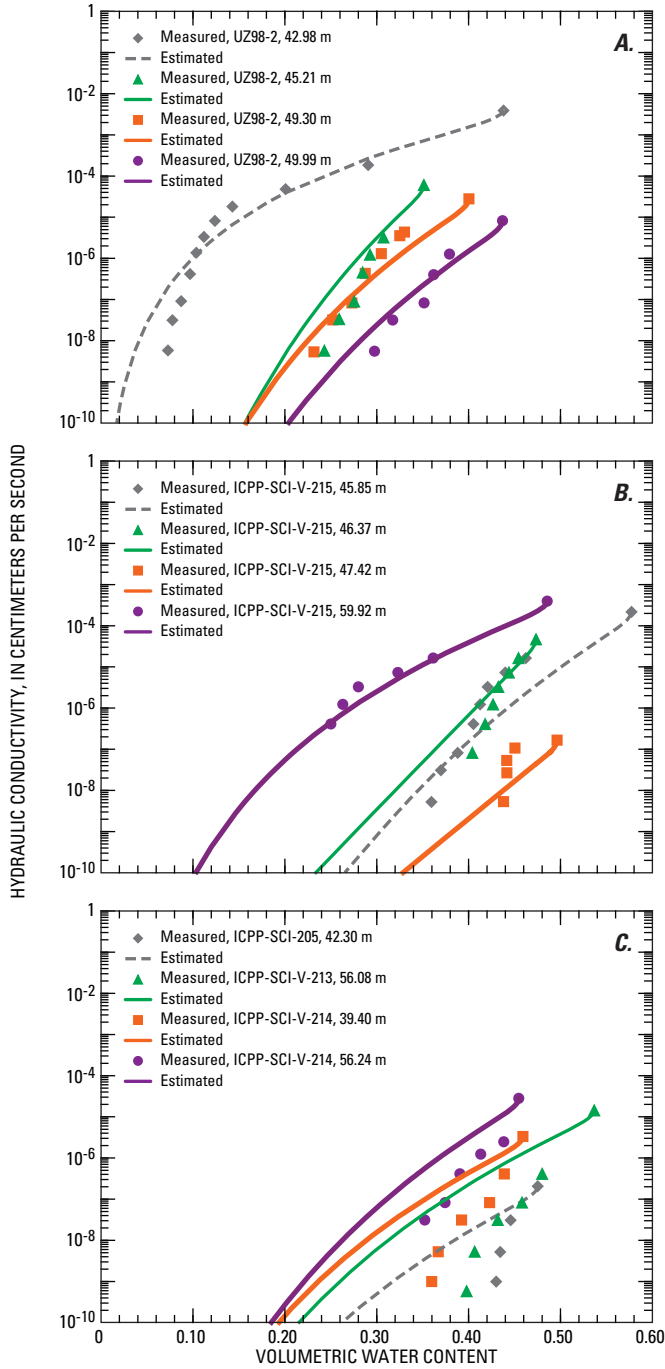


**Figure 9.** Unsaturated hydraulic conductivity curves estimated using the RNJ-CF model (laboratory-measured saturated hydraulic conductivity and Rossi-Nimmo junction model curve fits to measured water retention). Graphs *A*, *B*, and *C* show four samples each from Perkins and Nimmo (2000), Perkins (2003), and Winfield (2003), respectively.

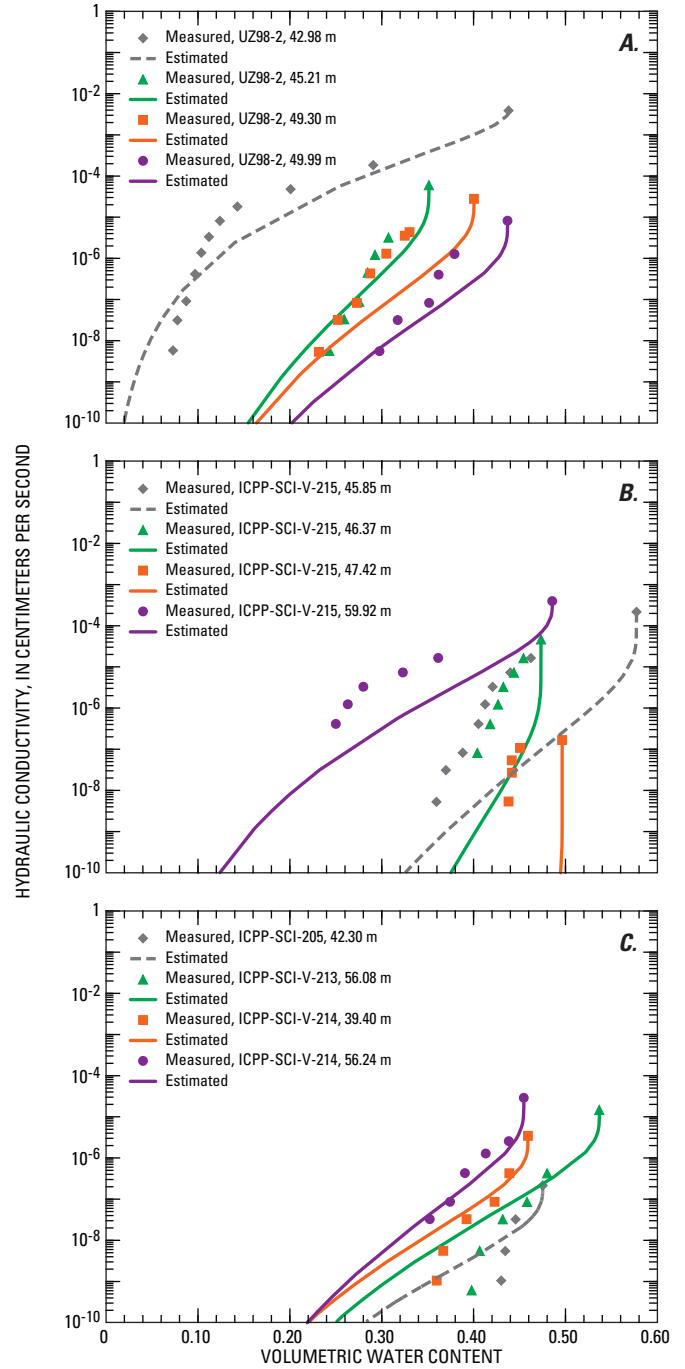


**Figure 10.** Unsaturated hydraulic conductivity curves estimated using the vG-CF model (laboratory-measured saturated hydraulic conductivity and van Genuchten model curve fits to measured water retention). Graphs *A*, *B*, and *C* show four samples each from Perkins and Nimmo (2000), Perkins (2003), and Winfield (2003), respectively.

A good estimate of  $K_{sat}$  does not necessarily improve the estimation of  $K(\theta)$  as might be expected because the  $K_{sat}$  value determines the position of the curve on the wet end. Although a well-estimated  $K_{sat}$  value anchors the curve near the true  $K_{sat}$  value on the wet end, it has no effect on the overall shape of the curve.

For several vG-CF  $K(\theta)$  estimates, the RMSE values were unusually large (fig. 11). This occurred in cases where few data points were available and the data clustered within a small range in  $\theta$ . The vG-CF model is not physically realistic for the entire range of  $\theta$  from saturation to  $\psi_d$  because the model uses  $\theta_r$  as an optimized parameter;  $\theta_r$  has no physical meaning. For the particular cases where no  $\theta(\psi)$  data are available in

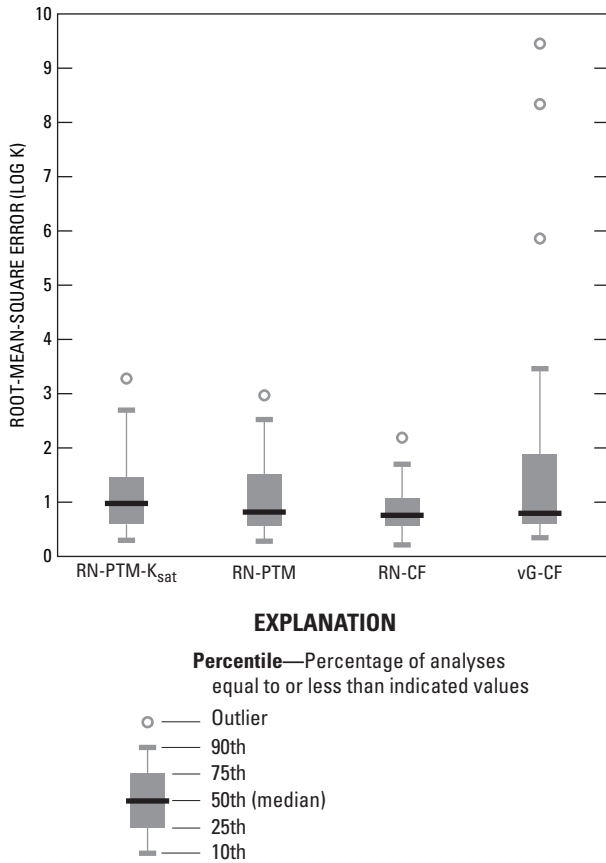


**Figure 11.** Comparison of root-mean-square errors in estimated hydraulic conductivity using RNJ-PTM- $K_{sat}$  model (property transfer model-estimated saturated hydraulic conductivity and Rossi-Nimmo junction model parameters); RNJ-PTM model (laboratory-measured saturated hydraulic conductivity and property transfer model-estimated Rossi-Nimmo junction model parameters); RNJ-CF model (laboratory-measured saturated hydraulic conductivity and Rossi-Nimmo junction model curve fits to measured water retention); and vG-CF model (laboratory-measured saturated hydraulic conductivity and van Genuchten model curve fits to measured water retention).

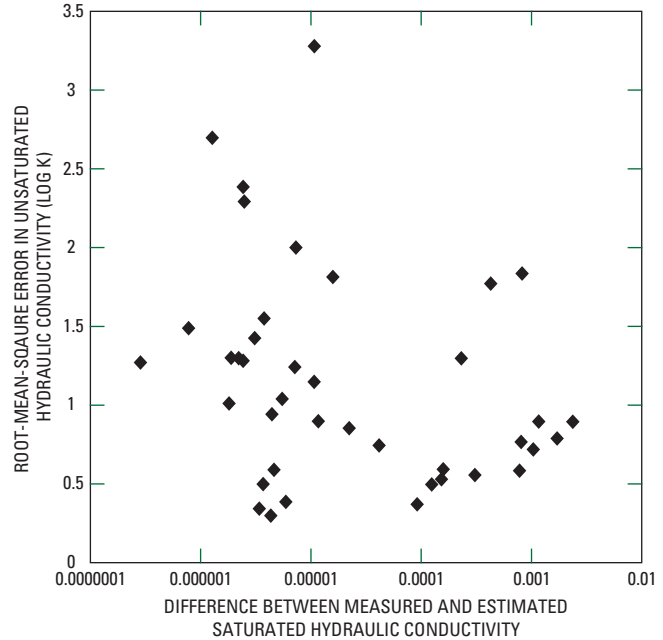


**Figure 12.** Comparison between unsaturated hydraulic conductivity estimates from property-transfer models in terms of root-mean-square error and saturated hydraulic conductivity in terms of difference between measured and estimated values.

the dry range and the measured points slope steeply within a small range in  $\theta$ , the curve asymptotically approaches  $\theta_r$ , starting from near  $\theta_{sat}$  (fig. 13A). On the resulting  $K(\theta)$  curve,  $K$  decreases sharply with little change in  $\theta$  (fig. 13B). The  $\theta(\psi)$  curve represented by the RNJ model goes to zero  $\theta$  at a fixed value of  $\psi$  calculated for the conditions of  $\psi_d$ ; therefore, even when few data points are available, the relation remains somewhat realistic and, in turn, allows for a better estimate of  $K(\theta)$ .

The PTMs developed by Winfield (2005) were evaluated in terms of the RMSE between RNJ-fit and RNJ PTM-estimated curves for the entire range from saturation to  $\psi_d$  rather than in terms of the RMSE between measured and estimated points. In evaluating  $K(\theta)$  estimates for this study, RMSE values were calculated between measured and estimated  $K(\theta)$  data points rather than curves because fits to measured  $K(\theta)$  data points are often poor. There appears to be no correlation between the RMSE values for  $\theta(\psi)$  curves and the RMSE values for RNJ-PTM- $K_{sat}$ -estimated  $K(\theta)$  data points (fig. 14). A good estimate of  $\theta(\psi)$  does not necessarily improve the estimate of  $K(\theta)$  because  $\theta(\psi)$  and  $K(\theta)$  are not always related as described by the mathematical formulas used in this study.

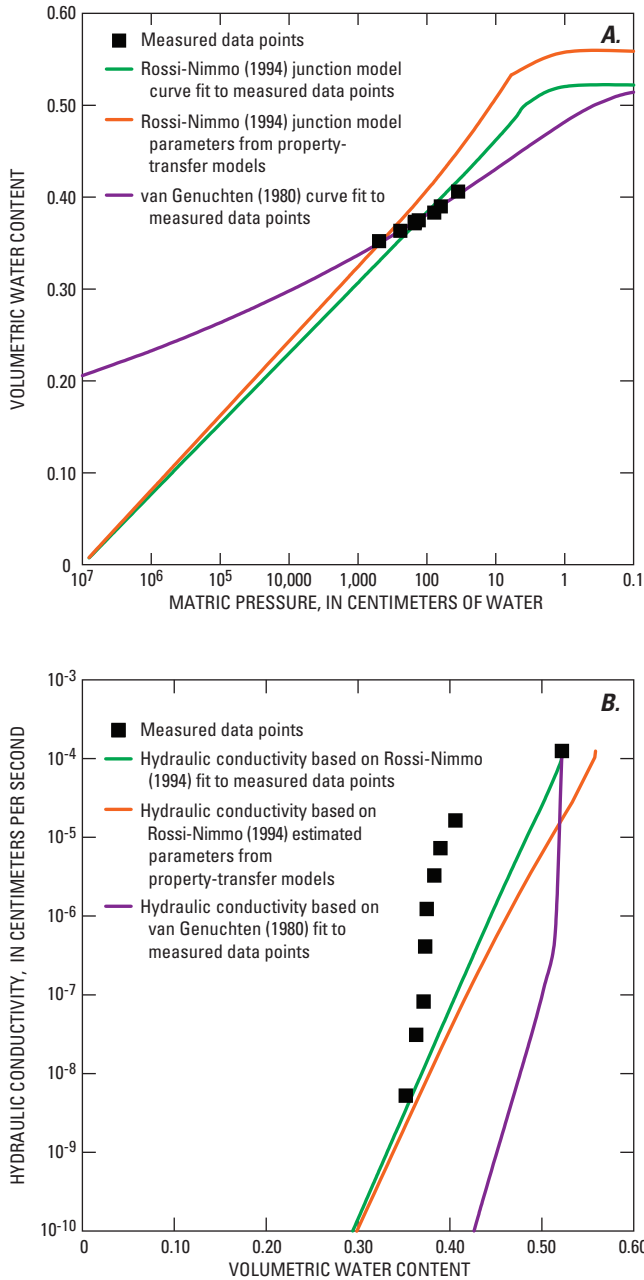


**Figure 13.** Water retention (A) and hydraulic conductivity (B) curves for core sample ICPP-SCI-V-215 (59.70 meter) illustrating the effect of few, clustered water-retention data points on the estimation of hydraulic conductivity.

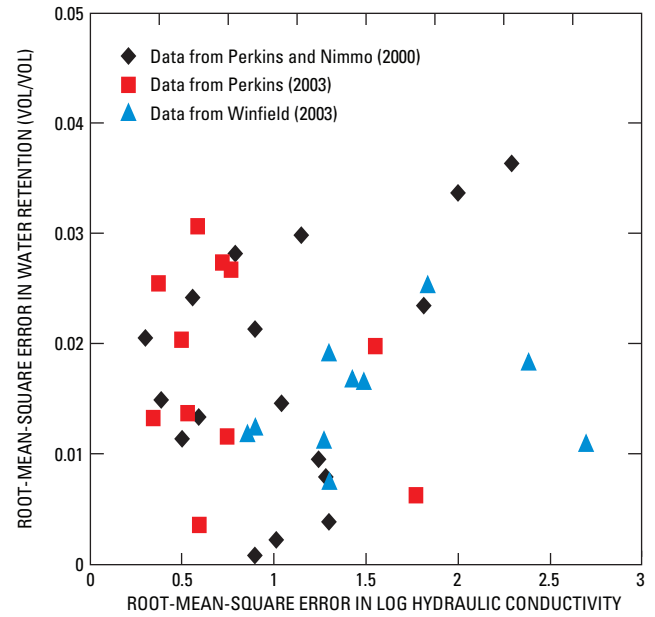


**Figure 14.** Comparison between goodness-of-fit of estimated water retention and goodness-of-fit of estimated unsaturated hydraulic conductivity in terms of root-mean-square error.

### Parameter Testing With Numerical Simulation

Development of a PTM to estimate  $K(\theta)$  is important for regional unsaturated-flow models where data do not exist for every point in space. Parameterized  $\theta(\psi)$  and  $K(\theta)$  curves, representative of the modeled media, are required input. For this study, numerical simulations were run to evaluate the effect of the input parameters on modeled results. Parameterized unsaturated hydraulic properties [ $K(\theta)$  and  $\theta(\psi)$ ] and the USGS variably saturated two-dimensional transport model (VS2DT) were used to simulate flow within a sedimentary interbed (Lappala and others, 1983; Healy, 1990; Hsieh and others, 1999) to evaluate the effect of the chosen input parameters. The model was modified to allow for the use of the Rossi-Nimmo water-retention parameters (R.W. Healy, U.S. Geological Survey, oral commun. 2006). VS2DT solves the finite-difference approximation to Richards' equation (Richards, 1931) for flow and the advection-dispersion equation for transport. The flow equation is written with total hydraulic potential as the dependent variable to allow straightforward treatment of both saturated and unsaturated conditions. Several boundary conditions specific to unsaturated flow, including ponded infiltration, specified fluxes in or out, seepage faces, evaporation, and plant transpiration, may be used. As input, the model requires saturated hydraulic conductivity, porosity, parameterized unsaturated hydraulic conductivity and water-retention functions, grid delineation, and initial hydraulic conditions.

Simulations based on properties for two core samples (58.6 m and 59.2 m) from borehole ICPP-SCI-V-215 located at the VZRP are presented in this report. Of the eight simulations, four are one-layer and four are two-layer systems each representing a single sedimentary interbed.  $\theta(\psi)$  was represented by functions developed by Rossi and Nimmo (1994) and van Genuchten (1980), in all cases using Mualem’s (1976) model to calculate  $K(\theta)$ . Parameters for each of these functions were obtained by property-transfer modeling or curve fitting, as described previously in this report. The unsaturated-flow properties of the one- and two-layer systems were characterized using RNJ-PTM- $K_{sat}$ , RNJ-PTM, RNJ-CF, and vG-CF model parameters (table 4) for a total of eight simulations.

The 1- by 1-m domain was discretized into 1- by 1-cm grid blocks with a boundary condition chosen to simulate 5 days of saturated infiltration within a 10-cm section at the top left of the domain. Initial hydraulic conditions were specified as uniform pressure head.

$\theta(\psi)$  and  $K(\theta)$  curves used as input for the one- and two-layer systems are shown in figure 15. RMSE values for  $\theta(\psi)$  and  $K(\theta)$  used to describe the sedimentary material in the simulations are given in table 5. The RMSE values for  $\theta(\psi)$  were calculated on basis of differences between laboratory-measured  $\theta(\psi)$  data points and estimated  $\psi$  values for the given  $\theta$  to allow for direct comparison between the RNJ-PTM, RNJ-CF, and vG-CF models.

**Table 4.** Parameter values used in numerical simulations for the one- and two-layer systems.

[**Abbreviations:** RNJ-PTM- $K_{sat}$ , property-transfer model-estimated saturated hydraulic conductivity and Rossi-Nimmo junction model parameters; RNJ-PTM, laboratory-measured saturated hydraulic conductivity and property-transfer model-estimated Rossi-Nimmo junction model parameters; RNJ-CF, laboratory-measured saturated hydraulic conductivity and Rossi-Nimmo junction model curve fits to measured water retention; vG-CF, laboratory-measured saturated hydraulic conductivity and van Genuchten model curve fits to measured water retention; cm<sup>3</sup>/cm<sup>3</sup>, cubic centimeter per cubic centimeter; cm-water, centimeter of water; cm/d, centimeter per day]

Layer	Water-retention parameters			Saturated hydraulic conductivity, $K_{sat}$ (cm/d)
	Saturated water content, $\theta_{sat}$ (cm <sup>3</sup> /cm <sup>3</sup> )	Scaling parameter for matric pressure, $\psi_0$ (cm-water)	Curve-shape parameter, $\lambda$	
RNJ-PTM- $K_{sat}$				
1	0.53	12.0	0.31	33.0
2	.49	26.0	.20	6.2
RNJ-PTM				
1	0.53	12.0	0.31	122.8
2	.49	26.0	.20	14.1
RNJ-CF				
1	0.57	3.6	0.22	122.8
2	.53	75.4	.31	14.1
vG-CF				
Scaling parameter for matric pressure, $\alpha$ (1/cm-water)				
Curve-shape parameter, $n$				
vG-CF				
1	0.57	0.28	1.22	122.8
2	.53	.01	1.38	14.1



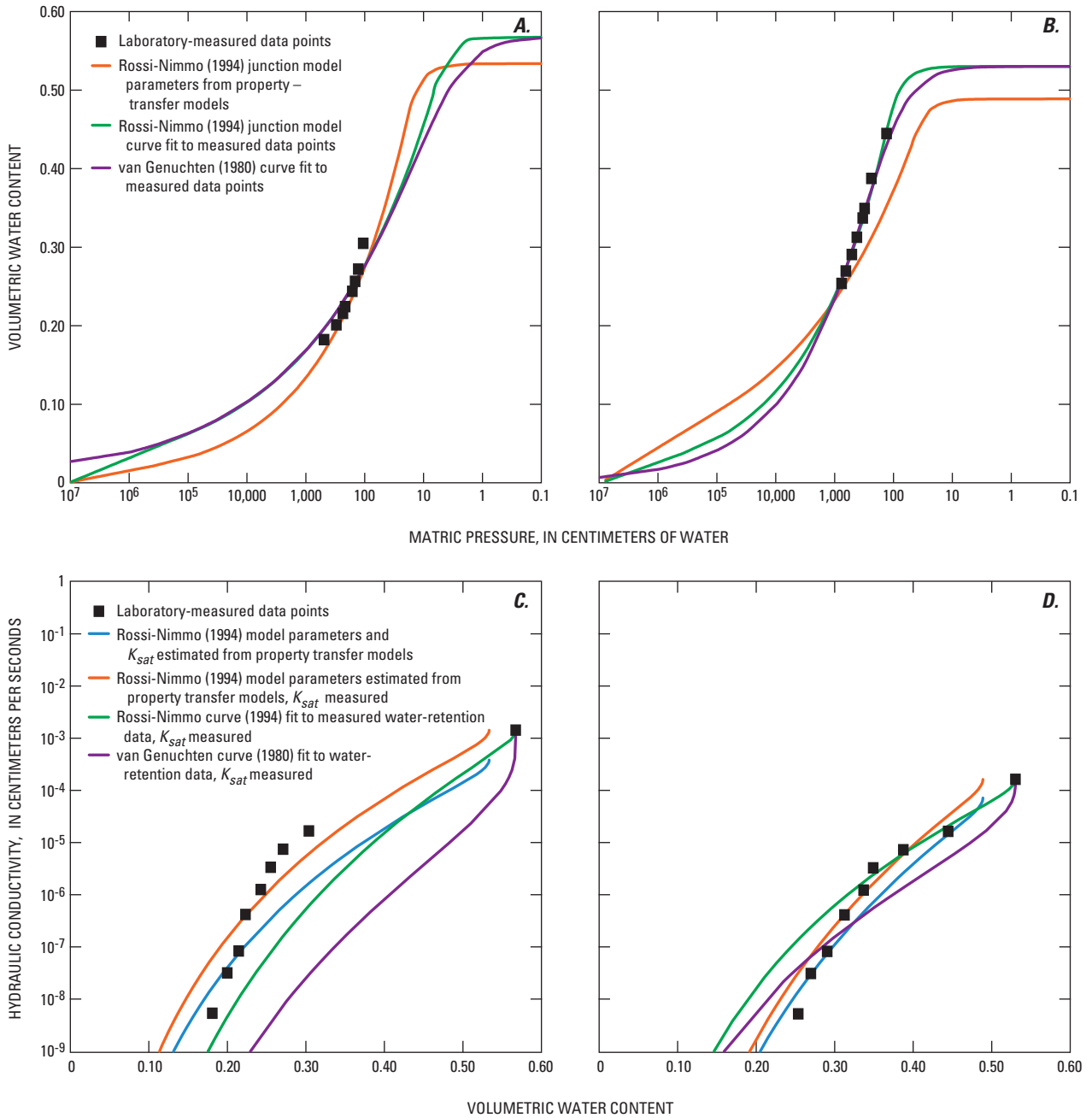


**Figure 15.** Water-retention (A is layer 1, B is layer 2) and hydraulic-conductivity (C is layer 1, D is layer 2) curves used in numerical simulations.

**Table 5.** Root-mean-square error values for water retention and hydraulic conductivity used to describe sedimentary interbed material in numerical simulations for a one- and two-layer system.

[**Abbreviations:** RNJ-PTM- $K_{sat}$ , property-transfer model-estimated saturated hydraulic conductivity and Rossi-Nimmo model parameters; RNJ-PTM, laboratory-measured saturated hydraulic conductivity and property-transfer model-estimated Rossi-Nimmo model parameters; RNJ-CF, laboratory-measured saturated hydraulic conductivity and Rossi-Nimmo model curve fits to measured water retention; vG-CF, laboratory-measured saturated hydraulic conductivity and van Genuchten model curve fits to measured water retention; RMSE, root-mean-square error;  $K(\theta)$ , unsaturated hydraulic conductivity;  $\theta(\psi)$ , water retention]

Layer	RNJ-PTM- $K_{sat}$	RNJ-PTM	RNJ-CF	vG-CF
RMSE $K(\theta)$ in units of log $K$				
1	0.72	0.56	1.29	2.60
2	.37	.36	.67	.57
RMSE $\theta(\psi)$ in units of volumetric water content				
1	0.01	0.01	0.02	0.10
2	.01	.01	.02	.14

Simulation results for all cases are presented in [figure 16](#). The images show the  $\theta$  distribution at the end of the 5-day simulation period. The results for the RNJ-PTM- $K_{sat}$  and RNJ-PTM model simulations are qualitatively the most similar for the one- and two-layer systems where the only difference in the input parameters is the  $K_{sat}$  values. The lower  $K_{sat}$  values ([table 4](#)) estimated for the RNJ-PTM- $K_{sat}$  model shifts the  $K(\theta)$  curve toward higher  $\theta$  for a given  $K$  relative to the curve for the RNJ-PTM model ([fig. 15C](#)). The effect of this shift is apparent in the slightly larger and more diffuse wetted area for the RNJ-PTM model simulations, primarily for the layer-1 material where the  $K_{sat}$  is substantially higher. For the RNJ-CF model simulations, there is less horizontal and more vertical flow within the layer-1 material than in the RNJ-PTM- $K_{sat}$  and RNJ-PTM model simulations. The RNJ-CF model parameters for layer 1 include a high  $K_{sat}$  value combined with a low  $\psi_o$  value, which tends to promote vertical flow and decrease the driving force (suction) for horizontal flow. The RNJ-CF model shifts the  $K(\theta)$  curve toward higher  $\theta$  for a given  $K$  in layer 1 ([fig. 15C](#)). The simulations using the vG-CF model parameters result in a much smaller wetted area in both cases, probably

because of the large decrease in  $K$  with very little change in  $\theta$  near the wet end of the  $K(\theta)$  curve ([fig. 15C](#) and [D](#)). This artifact, which is the main difference in the curve shapes, may have been the cause of an apparent reduction in computational efficiency. The simulations using vG-CF model parameters required several hours, whereas the simulations using the RNJ model parameters required only several minutes.

The simulation results shown in [figure 16](#) illustrate the effect of the model parameters by a comparison among methods. The only indication of which simulations come closest to reality is based on laboratory-measured hydraulic properties and the calculated RMSE values ([table 5](#)). The RNJ-PTM model estimates yielded the lowest RMSE values. If the RNJ-PTM model simulations are assumed to be the most accurate, then the RNJ-PTM- $K_{sat}$  model simulations match most closely. However, in some cases, using the RMSE values in this type of evaluation can be misleading; the RMSE is the error calculated for the entire range of points whereas the simulation may be most affected by the nature of the wet end of the curves.

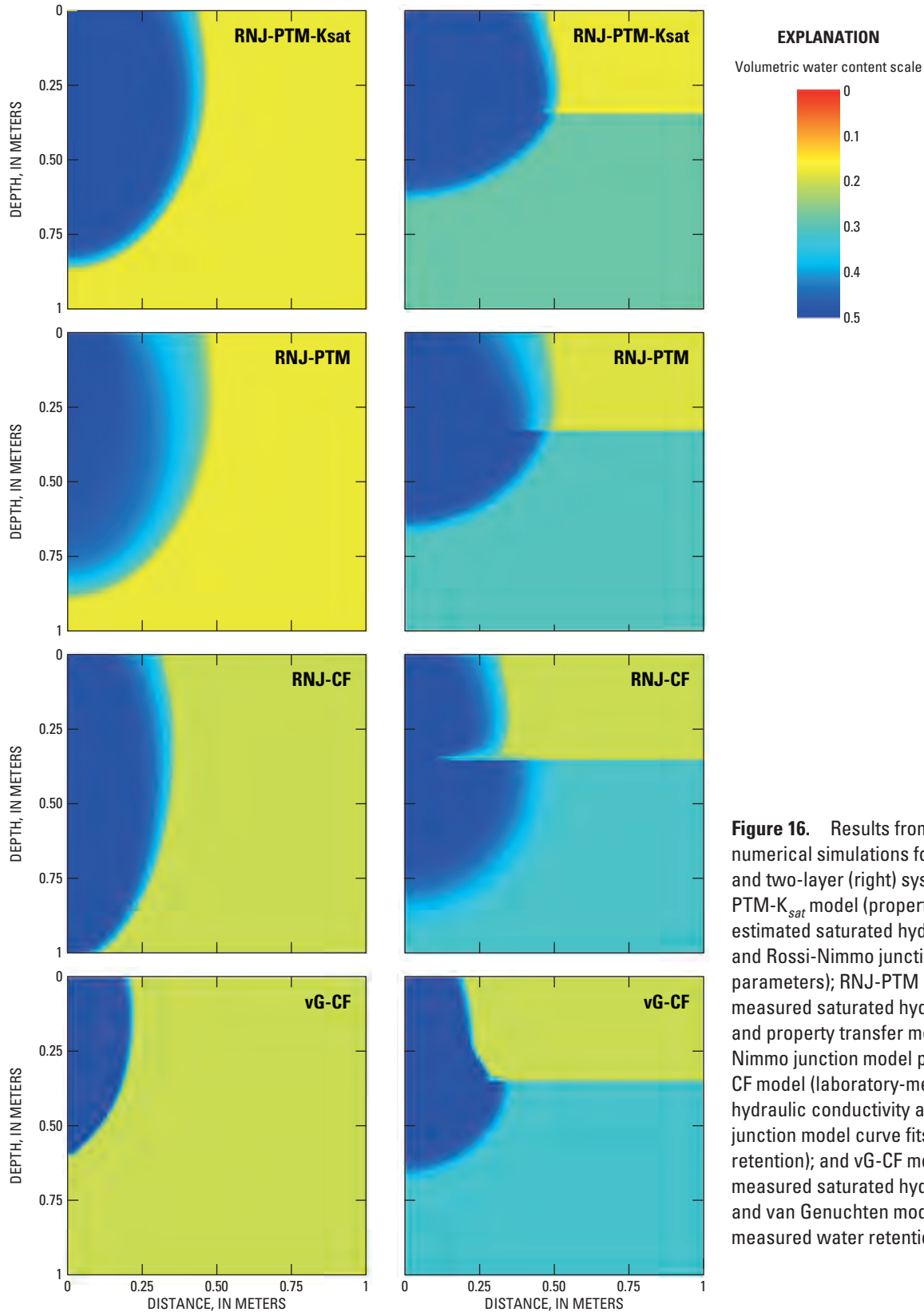


**Figure 16.** Results from VS2DT model numerical simulations for one-layer (left) and two-layer (right) systems using RNJ-PTM- $K_{sat}$  model (property transfer model-estimated saturated hydraulic conductivity and Rossi-Nimmo junction model parameters); RNJ-PTM model (laboratory-measured saturated hydraulic conductivity and property transfer model-estimated Rossi-Nimmo junction model parameters); RNJ-CF model (laboratory-measured saturated hydraulic conductivity and Rossi-Nimmo junction model curve fits to measured water retention); and vG-CF model (laboratory-measured saturated hydraulic conductivity and van Genuchten model curve fits to measured water retention).

## Summary and Conclusions

Property-transfer models (PTMs) developed for sedimentary interbeds at the Idaho National Laboratory were combined with a capillary-bundle model to estimate unsaturated hydraulic conductivity [ $K(\theta)$ ]. The site-specific property-transfer models were developed to estimate saturated hydraulic conductivity ( $K_{sat}$ ) and the three parameters that define the water-retention curves [ $\theta(\psi)$ ] using the Rossi-Nimmo junction (RNJ) model [saturated water content ( $\theta_{sat}$ ), a scaling parameter for matric pressure ( $\psi_o$ ), and a curve-shape parameter ( $\lambda$ )] from more easily-measured bulk density and particle-size distributions. The RNJ model was integrated with Mualem's capillary-bundle model for  $K(\theta)$ .  $\theta(\psi)$  and  $K(\theta)$  are required as input in numerical models of variably-saturated flow and transport which are commonly-used tools in risk assessment.

$K(\theta)$  was calculated using (1) PTM-estimated  $K_{sat}$  and PTM-estimated RNJ model parameters (RNJ-PTM- $K_{sat}$ ), (2) laboratory-measured  $K_{sat}$  and PTM-estimated RNJ model parameters (RNJ-PTM), (3) laboratory-measured  $K_{sat}$  and RNJ model curve fits to measured  $\theta(\psi)$  data points (RNJ-CF), and (4) laboratory-measured  $K_{sat}$  and van Genuchten model curve fits to measured  $\theta(\psi)$  data points (vG-CF). The root-mean-square errors between laboratory-measured and model-estimated values of  $K(\theta)$  for 40 samples were compared to evaluate the performance of the PTMs in estimating  $K(\theta)$ . The PTMs performed well;  $K$  was equally well predicted by either the RNJ-PTM- $K_{sat}$  or RNJ-PTM models as by the RNJ-CF model and better overall than the vG-CF model. The RNJ-PTM- $K_{sat}$  and RNJ-PTM models performed almost equally well, supporting the value of the Winfield (2005) PTMs. Direct measurement of  $K_{sat}$  may not appreciably improve the estimation capability of the  $\theta(\psi)$  PTMs. Another significant conclusion is that in 25 of the 40 cases,  $K$  was better predicted by the RNJ-CF model than by the vG-CF model, most likely because of the more physically realistic nature of the RNJ model. Interestingly, there is no correlation between goodness of  $\theta(\psi)$  estimation and goodness of  $K(\theta)$  estimation nor is there a correlation between goodness of  $K_{sat}$  estimation and goodness of  $K(\theta)$  estimation.

Because PTMs commonly are used to derive input for ground-water flow and transport models, numerical simulations were run to illustrate the influence of the parameters on simulated results by allowing a comparison among methods. Conclusions drawn from this exercise are useful, though limited. The only indication as to which simulation approximates reality most closely is based on knowledge of laboratory-measured hydraulic properties and the computed root-mean-square error values, where the RNJ-PTM model estimations yielded the lowest values. RNJ-PTM- $K_{sat}$  model simulation results are qualitatively the most similar to the RNJ-PTM model simulation results. However, using

root-mean-square error values in this type of evaluation can be misleading as the error is calculated for the entire range of points whereas the simulation may be most affected by the nature of the wet end of the curves.

A limitation to the practical application of the PTMs is that the core samples used to develop them are texturally limited; high clay and gravelly samples are underrepresented. However, the property-transfer models do afford the opportunity to estimate hydraulic properties of the sedimentary interbeds over greater depths and distances than would otherwise be possible.

## Acknowledgments

The authors would like to thank Joseph Rousseau, U.S. Geological Survey, for his continued support and encouragement during this project.

## References Cited

- Anderson, S.R., 1991, Stratigraphy of the unsaturated zone and uppermost part of the Snake River Plain aquifer at the Idaho Chemical Processing Plant and Test Reactor Area, Idaho National Engineering Laboratory, Idaho: U.S. Geological Survey Water-Resources Investigations Report 91-4010 (DOE/ID-22095), 71 p.
- Anderson, S.R., and Lewis, B.D., 1989, Stratigraphy of the unsaturated zone at the Radioactive Waste Management Complex, Idaho National Engineering Laboratory, Idaho: U.S. Geological Survey Water-Resources Investigations Report 89-4065 (DOE/ID-22080), 54 p.
- Anderson, S.R., Liszewski, M.J., and Ackerman, D.J., 1996, Thickness of surficial sediment at and near the Idaho National Engineering Laboratory, Idaho: U.S. Geological Survey Open-File Report 96-330 (DOE/ID-22128), 16 p.
- Andraski, B.J., 1996, Properties and variability of soil and trench fill at an arid waste-burial site: Soil Science Society of America Journal, v. 60, p. 54-66.
- Andraski, B.J., and Jacobson, E.A., 2000, Testing a full-range soil-water retention function in modeling water potential and temperature: Water Resources Research, v. 36, no. 10, p. 3081-3089.
- Barraclough, J.T., Lewis, B.D., and Jensen, R.G., 1981, Hydrologic conditions at the Idaho National Engineering Laboratory, Idaho—Emphasis 1974-1978: U.S. Geological Survey Water-Supply Paper 2191, 52 p.

- Barracough, J.T., Teasdale, W.E., and Jensen, R.G., 1967, Hydrology of the National Reactor Testing Station area, Idaho—Annual progress report, 1965: U.S. Geological Survey Open-File Report (IDO-22048), 107 p.
- Brooks, R.H., and Corey, A.T., 1964, Hydraulic properties of porous media: Colorado State University Hydrology Paper, no. 3, 27 p.
- Fayer, M.J., Rockhold, M.L., and Campbell, M.D., 1992, Hydrologic modeling of protective barriers—Comparison of field data and simulation results: *Soil Science Society of America Journal*, v. 56, p. 690–700.
- Hackett, B., Pelton, J., and Brockway, C., 1986, Geohydrologic story of the eastern Snake River Plain and the Idaho National Engineering Laboratory: U.S. Department of Energy, Idaho Operations Office, Idaho National Engineering Laboratory, 32 p.
- Healy, R.W., 1990, Simulation of solute transport in variably saturated porous media with supplemental information on modifications to the U.S. Geological Survey's computer program VS2DT: U.S. Geological Survey Water-Resources Investigations Report 90-4025, 125 p.
- Hsieh, P.A., Wingle, W., and Healy, R.W., 1999, VS2DTI—A graphical user interface for the variably saturated flow and transport computer program VS2DT: U.S. Geological Survey Water-Resources Investigations Report 99-4130, 13 p.
- Lappala, E.G., Healy, R.W., and Weeks, E.P., 1983, Documentation of the computer program VS2D to solve the equations of fluid flow in variably saturated porous media: U.S. Geological Survey Water-Resources Investigations Report 83-4099, 184 p.
- Liszewski, M.J., and Mann, L.J., 1992, Purgeable organic compounds in ground water at the Idaho National Engineering Laboratory, Idaho—1990 and 1991: U.S. Geological Survey Open-File Report 92-174 (DOE/ID-22104), 19 p.
- McElroy, D.L., and Hubbell, J.M., 1990, Hydrologic and physical properties of sediments at the Radioactive Waste Management Complex: EG&G Idaho, Inc., EGG-BG-9147, [variously paged].
- Mualem, Y., 1976, A new model for predicting the hydraulic conductivity of unsaturated porous media: *Water Resources Research*, v. 12, no. 3, p. 513–522.
- Perkins, K.S., 2003, Measurement of sedimentary interbed hydraulic properties and their hydrologic influence near the Idaho Nuclear Technology and Engineering Center at the Idaho National Engineering and Environmental Laboratory: U.S. Geological Survey Water-Resources Investigations Report 03-4048 (DOE/ID-22183), 19 p.
- Perkins, K.S., and Nimmo, J.R., 2000, Measurement of hydraulic properties of the B-C interbed and their influence on contaminant transport in the unsaturated zone at the Idaho National Engineering and Environmental Laboratory, Idaho: U.S. Geological Survey Water-Resources Investigations Report 00-4073 (DOE/ID-22170), 30 p.
- Richards, L.A., 1931, Capillary conduction of liquids through porous media: *Physics*, v. 1, p. 318–333.
- Rightmire, C.T., and Lewis, B.D., 1987, Hydrogeology and geochemistry of the unsaturated zone, Radioactive Waste Management Complex, Idaho National Engineering Laboratory, Idaho: U.S. Geological Survey Water-Resources Investigations Report 87-4198 (DOE/ID-22073), 89 p.
- Ross, P.J., Williams, J., and Bristow, K.L., 1991, Equation for extending water-retention curves to dryness: *Soil Science Society of America Journal*, v. 55, p. 923–927.
- Rossi, C., and Nimmo, J.R., 1994, Modeling of soil water retention from saturation to oven dryness: *Water Resources Research*, v. 30, no. 3, p. 701–708.
- Soil Survey Staff, 1975, Soil taxonomy—a basic system of soil classification for making and interpreting soil surveys: Washington, D.C., USDA-SCS Agriculture Handbook no. 436, U.S. Government Printing Office, 754 p.
- van Genuchten, M.Th., 1980, A closed-form equation for predicting the hydraulic conductivity of unsaturated soils: *Soil Science Society of America Journal*, v. 44, p. 892–898.
- Winfield, K.A., 2003, Spatial variability of sedimentary interbed properties near the Idaho Nuclear Technology and Engineering Center at the Idaho National Engineering and Environmental Laboratory, Idaho: U.S. Geological Survey Water-Resources Investigations Report, 03-4142, 36 p.
- Winfield, K.A., 2005, Development of property-transfer models for estimating the hydraulic properties of deep sediments at the Idaho National Engineering and Environmental Laboratory, Idaho: U.S. Geological Survey Scientific Investigations Report 2005-5114 (DOE/ID-22196), 49 p.

This page intentionally left blank.

Manuscript approved for publication, May 15, 2007.

Prepared by the USGS Publishing Network

Bill Gibbs

Bob Crist

Bobbie Jo Richey

Cathy Martin

Sharon Wahlstrom

For more information concerning the research in this report, contact the

Director, Idaho Water Science Center

230 Collins Road

Boise, Idaho 83702-4520

<http://id.water.usgs.gov>

